UNIVERSITY OF THESSALY
SCHOOL OF ENGINEERING
DEPARTMENT OF MECHANICAL ENGINEERING

Diploma Thesis

Thermal and stress analysis of a two-dimensional additive manufacturing process

by
CHARALAMPOPOULOS PANTELIS

Submitted in Partial Fulfilment of the Requirements for Diploma in
Mechanical Engineering 2021

Approved by the Three Members of the Advisory Committee:

First member (Supervisor)

Professor Nikolaos Aravas
Department of Mechanical Engineering, University of Thessaly

Second member

Adjunct Professor Ioanna Papadioti
Department of Mechanical Engineering, University of Thessaly

Third member

Professor Giorgos Liberopoulos
Department of Mechanical Engineering, University of Thessaly

Abstract

Additive manufacturing (AM) is the construction of a three-dimensional object from a digital 3D model, with material being added together, layer by layer. The high temperature process will produce large tensile residual stresses which lead to part distortion and negatively affect product performance. In AM an accurate estimation of residual stresses and distortion is necessary to achieve dimensional accuracy and prevent bad product performance. In this work, an integrated thermomechanical simulation of additive manufacturing process, as applied to an AISI 316L austenitic stainless steel, is presented. A finite element technique is employed to evaluate the temperature evolution as well as residual stresses and distortions in the processed part, due to the successive material deposition. In particular, an one-way coupled analysis is carried out with the heat transfer and mechanical problems solved in sequence. The material deposition is modeled using elements which are activated as the added material solidifies. These elements are present from the start of the analysis but are assigned properties so they do not affect the analysis. The ensuing temperature field is then provided as an input for the mechanical analysis, to calculate the residual stresses and distortions. The current implementation is for two-dimensional models but can be extended to three-dimensional cases.

Contents

List of Figures

List of Tables

Introduction

Additive manufacturing (AM), is the construction of a three-dimensional object from a digital 3D model, with material being added together, layer by layer. More specific, a powder delivering system is used to place a thick powder layer every time. Then a laser is used to heat and melt the metal powder, which later solidifies to form a fully dense layer. The addition of multiple layers can produce a three dimensional fully dense part.

This construction process is very useful due to its ability to easily design and build parts with complex geometries, which the traditional manufacturing constraints, such as tooling and physical access to surfaces for machining, could not allow. The technology is used both for rapid prototyping, as it decreases the time needed to develop new products, and production manufacturing, as a cost saving method to simplify assemblies and complex geometries and to reduce the material waste. Thus, it is used mainly in industries that have small to medium size, highly complex parts, such as aerospace, dental and medical.

As it is described earlier, AM process involves heating, melting and solidification of a metal, by a moving source, such as a laser in a layer by layer manner. As a consequence, different regions of the work piece experience repeated heating and cooling, which results in a high temperature gradient, that generates thermal stresses and leads to cracks and part distortion.

Part distortion due to residual stresses is one of the major defects of AM parts. So, an accurate estimation of residual stresses and distortion is necessary to achieve dimensional accuracy and prevent an unexpected component failure. Since AM is affected by a variety of variables, an experimental measurement of residual stresses and distortion is time consuming and expensive. Therefore, numerical thermo-mechanical models can be used for their estimation, but the quality of the calculations depends critically on the accurate transient temperature field, which affects both the residual stresses and dis-

tortion.

As the laser hits the work piece surface, the powder melts quickly to form a molten pool. During the melting process, energy and mass transformation occurs through various physical phenomena, such as absorption and scattering of laser radiation, heat transfer and fluid flow within the molten pool. Simulation of these complex physical processes is computationally intensive and in order to build a computationally viable model, simplifications and assumptions of these processes are necessary. These include several two-dimensional models [3, 4] or an assumption that the entire deposit is heated and then cooled [5] or building a part by a single layer deposition [6]. However, it is very important to avoid making assumptions that may lead to miscalculations of the temperature field, because it is critical to calculate an accurate transient temperature field. It has been shown [7, 8] that ignoring the surface convection and radiation leads to the calculation of inaccurate temperature fields.

In this work, an integrated thermomechanical simulation of additive manufacturing process, as applied to an AISI 316L austenitic stainless steel, is presented. A finite element technique is employed to evaluate the temperature evolution as well as residual stresses and distortions in the processed part, due to the successive material deposition. In particular, an one-way coupled analysis is carried out with the heat transfer and mechanical problems solved in sequence. The material deposition is modeled using elements which are activated as the added material solidifies. These elements are present from the start of the analysis but are assigned properties so they do not affect the analysis. This technique is similar to the quiet element method, as it was presented here [9]. The ensuing temperature field is then provided as an input for the mechanical analysis, to calculate the residual stresses and distortions. The current implementation is for two-dimensional models but can be extended to three-dimensional cases. In order to develop this simulation, finite element analysis (FEA) package ABAQUS [1] was used.

This thesis proceeds with Chapter 1, where we present the necessary theoretical background, that is the heat transfer and the continuum mechanics theory. Having the fundamentals set, we proceed with Chapter 2, where we describe the development of the finite element model both for the thermal and mechanical analysis, implementing the relationships of Chapter 1 and new methods, such as the modified-quiet element method, in order to simulate the AM process. In Chapter 3, we present the thermomechanical simulation of additive manufacturing process, as applied to an AISI 316L

austenitic stainless steel. Finally, in 3.2 we summarize the results, make some conclusions and propose some improvements to enhance the model.

Chapter 1

Theory

1.1 Heat Transfer

Heat is the form of energy that can be transferred from one system to another as a result of temperature difference. Heat transfer refers to the rate of such energy transfers, which depends upon the differences in temperature, the greater the difference in temperature, the greater the rate of heat transfer. Most of the relationships that follow based on the [10, 11].

As it is described earlier, temperature difference is the driving force of heat transfer, while the medium, which heat travels through from one body to another, is the resistance to the heat flow. Both of these factors, affect the rate of heat transfer, as we can see in the following general equation for heat transfer:

[rate of heat transfer] = [temperature difference]/[resistance]

During heat transfer, temperatures can change, so the rate, also, will change. This is called unsteady-state heat transfer, in contrast with steady-state heat transfer, where the temperatures do not change and the rate remains constant.

Heat transfer is classified into various mechanisms, such as thermal conduction, thermal convection, thermal radiation, and transfer of energy by phase changes.

Heat conduction, also called diffusion, is the direct microscopic exchange of kinetic energy of particles through the boundary between two systems.

When an object is at a different temperature from another body or its surroundings, heat flows so that the body and the surroundings reach the same temperature. Such spontaneous heat transfer always occurs from a region of high temperature to another region of lower temperature, as described in the second law of thermodynamics.

Convection is the mode of heat transfer between a solid surface and the adjacent liquid or gas that is in motion, and it involves the combined effects of conduction and fluid motion.

Radiation is the energy emitted by matter in the form of electromagnetic waves as a result of the changes in the electronic configurations of the atoms or molecules.

In general, heat is transferred in solids by conduction, in fluids by conduction and convection. Heat transfer by radiation occurs through open space, can often be neglected, and is most significant when temperature differences are substantial. In practice, all the three types of heat transfer may occur together, while for calculations it is often better to consider the mechanisms separately, and then to combine them where it is necessary.

Although heat transfer ant temperature are closely related, they are of a different nature. Unlike temperature, heat transfer has direction as well as magnitude, and thus is a vector quantity. Therefore, we must specify both direction and magnitude in order to describe heat transfer completely at a point.

1.1.1 Heat Conduction

Heat conduction in a medium, in general, is three-dimensional and time dependent. That is, $T=T(x,y,z,t)$ and the temperature in a medium is said to be steady when the temperature does not vary with time and unsteady or transient when it does. Heat conduction in a medium is said to be one-dimensional when conduction is significant in one dimension only and negligible in the other two dimensions, two-dimensional when conduction in the third dimension is negligible, and three dimensional when conduction in all dimensions is significant.

Heat conduction through a medium in a specified direction is proportional to the temperature difference across the medium and the area normal to the direction of heat transfer, but is inversely proportional to the distance in that direction. This was expressed in the differential form by Fourier's law of heat

conduction for one-dimensional heat conduction as:

$$\dot{Q}_{cond} = -kA\frac{dT}{dx} \qquad (W) \tag{1.1}$$

where k is the thermal conductivity[1] of the material, which is a measure of the ability to conduct heat, dT/dx is the temperature gradient, which is the slope of the temperature curve on a T-x diagram, and A is the heat conduction area normal to the x-direction. The thermal conductivity of a material, in general, varies with temperature, but sufficiently accurate results can be obtained by using a constant value for thermal conductivity at the average temperature.

Heat is conducted in the direction of decreasing temperature, and thus the temperature gradient is negative when heat is conducted in the positive x-direction. The negative sign in Eq: 1.1 ensures that heat transfer is conducted in the positive x-direction is a positive quantity.

To obtain a general relation for Fourier's law of heat conduction, consider a medium in which the temperature distribution is three-dimensional. In rectangular coordinates, the heat conduction vector of a point P on the surface in that medium, can be expressed as:

$$\vec{\dot{Q}}_n = \dot{Q}_x\vec{i} + \dot{Q}_y\vec{j} + \dot{Q}_z\vec{k} \tag{1.2}$$

where $\vec{i}, \vec{j}$, and $\vec{k}$ are the unit vectors, and $\dot{Q}_x, \dot{Q}_y$, and $\dot{Q}_z$ are the magnitudes of the heat transfer rates in the x-,y-, and z-directions, which again can be determined from Fourier's law as:

$$\dot{Q}_x = -kA_x\frac{dT}{dx}, \qquad \dot{Q}_y = -kA_y\frac{dT}{dy}, \qquad and \qquad \dot{Q}_z = -kA_z\frac{dT}{dz} \tag{1.3}$$

Here A_x, A_y and A_z are heat conductive areas normal to the x-,y-, and z-directions, respectively.

In anisotropic materials such as the fibrous or composite materials, the properties may change with direction. For example, some of the properties of wood along the grain are different than those in the direction normal to the

---

[1]Although commonly expressed as a scalar, the most general form of thermal conductivity is a second-rank tensor. However, the tensorial description only becomes necessary in materials which are anisotropic. This thesis refers to homogeneous isotropic materials

grain. In such cases the thermal conductivity may need to be expressed as a tensor quantity to account for the variation with direction. Most engineering materials are isotropic in nature, and thus they have the same properties in all directions. For such materials we do not need to be concerned about the variation of properties with direction and we can assume the thermal conductivity of a material to be independent of direction.

1.1.2 Heat Convection

Conduction and convection are similar in that both mechanisms require the presence of a material medium. But they are different in that convection requires the presence of fluid motion.

Convection is classified as natural (or free) and forced convection, depending on how the fluid motion is initiated. In forced convection, the fluid is forced to flow over a surface or in a pipe by external means such as a pump or a fan. In natural convection, any fluid motion is caused by natural means such as the buoyancy effect, which manifests itself as the rise of warmer fluid and the fall of the cooler fluid. Convection is also classified as external and internal, depending on whether the fluid is forced to flow over a surface or in a channel.

Heat transfer through a solid is always by conduction, since the molecules of a solid remain at relatively fixed positions. Heat transfer through a moving liquid or gas, is by convection. The rate of heat transfer through a fluid is much higher by convection than is by conduction. In fact the higher the fluid velocity, the higher the rate of heat transfer.

Convection heat transfer is complicated by the fact that it involves fluid motion as well as heat conduction. Despite the complexity of convection, the rate of convection heat transfer is observed to be proportional to the temperature difference and is conveniently expressed by Newton's law of cooling as:

$$\dot{Q}_{conv} = hA_s(T_s - T_\infty) \qquad (W) \tag{1.4}$$

where h is the convection heat transfer coefficient, A_s is the heat transfer area, T_s is the temperature of the surface, and T_∞ is the temperature of the fluid sufficiently far from surface.

Although, the appearance of this relation looks simple, the convection heat transfer coefficient h depends on several variables, such as dynamic viscosity μ, thermal conductivity k, density ρ, specific heat C_p and fluid velocity V, geometry and roughness of the solid surface, thus it is difficult to determine.

1.1.3 Thermal radiation

So far, we have considered the conduction and convection modes of heat transfer, which are related to the nature of the materials involved and the presence of fluid motion, among other things. The third mechanism of heat transfer: radiation, is characteristically different from the other two.
Radiation heat transfer is the transfer of heat energy by electromagnetic radiation. Radiation operates independently of the medium through which it occurs and depends upon the relative temperatures, geometric arrangements and surface structures of the materials that are emitting or absorbing heat. The basic formula for radiant-heat transfer is the Stefan-Boltzmann Law:

$$\dot{Q}_{rad} = A\sigma T^4 \qquad (W) \qquad (1.5)$$

where T is the absolute temperature (measured from the absolute zero of temperature at – 273°) in degrees Kelvin (K) in the SI system, and σ is the StefanBoltzmann constant = 5.73 x $10^{-8} Jm^{-2}s^{-1}K^{-4}$.
This law gives the radiation emitted by a perfect radiator, a black body, as this is called. A black body gives the maximum amount of emitted radiation possible at its particular temperature. Real surfaces at a temperature T do not emit as much energy as predicted by Eq: 1.5, but it has been found that many emit a constant fraction of it. For these real bodies, that emit a constant fraction of the radiation from a black body, the equation can be rewritten:

$$\dot{Q}_{rad} = \varepsilon A\sigma T^4 \qquad (W) \qquad (1.6)$$

where ε is called the emissivity of the particular body and is a number between 0 and 1, and varies with the temperature T and with the wavelength of the radiation emitted. Bodies obeying this equation are called grey bodies. Just as a black body emits radiation, it also absorbs radiation according to

Eq: 1.5. Again grey bodies absorb a fraction of the quantity that a black body would absorb, corresponding this time to their absorptivity α. For grey bodies it can be shown that $\alpha=\varepsilon$. The fraction of the incident radiation that is not absorbed is reflected, and thus, there is a further term used, the reflectivity, which is equal to $(1 - \alpha)$.

The radiant energy transferred between two surfaces depends upon their temperatures, the geometric arrangement, and their emissivities. For two parallel surfaces, facing each other and neglecting edge effects, each must intercept the total energy emitted by the other, either absorbing or reflecting it. In this case, the net heat transferred from the hotter to the cooler surface is given by:

$$\dot{Q}_{rad} = AC\sigma(T_1^4 - T_2^4) \qquad (W) \tag{1.7}$$

where $1/C = 1/\varepsilon_1 + 1/\varepsilon_2$ - 1, ε_1 is the emissivity of the surface at temperature T_1 and ε_2 is the emissivity of the surface at temperature T_2. Usually, it is considered that $\varepsilon_2 = 1$, so: $C=\varepsilon_1=\varepsilon$.

1.1.4 Heat generation

A medium through which heat is conducted may involve the conversion of electrical, nuclear, or chemical energy into heat (or thermal) energy. In heat conduction analysis, such conversion processes are characterized as heat generation.

A source of heat generation in a medium is exothermic or endothermic chemical reactions that may occur throughout the medium, the electric current passes through a resistance and the phase change of a substance.

Note that heat generation is a volumetric phenomenon. That is, it occurs throughout the body of a medium. Therefore, the rate of heat generation in a medium is usually specified per unit volume and is denoted by $\dot{g}$, whose unit is W/m^3. The rate of heat generation in a medium may vary with time as well as position within the medium. When the variation of heat generation with position is known, the total rate of heat generation in a medium of volume V can be determined from:

$$\dot{G} = \int_V \dot{g}\, dV \qquad (W) \tag{1.8}$$

1.1.5 Heat conduction equation

In many geometries, such as the wall of a house, heat conduction can be approximated as being one-dimensional since heat conduction through these geometries will be dominant in one direction and negligible in other directions.

One-dimensional heat conduction equation

Consider a thin element of thickness x in a large plane wall. Assume the density of the wall is ρ, the specific heat is C, and the area of the wall normal to the direction of heat transfer is A. An energy balance on this thin element during a small time interval t can be expressed as:

(rate of heat conduction at x) - (rate of heat conduction at x+Δx) + (rate of heat generation inside the element) = (rate of change of the energy content of the element)

or

$$\dot{Q}_x - \dot{Q}_{x+\Delta x} + \dot{G}_{element} = \frac{\Delta E_{element}}{\Delta t} \tag{1.9}$$
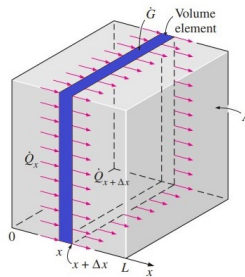
Figure (1.1)   One-dimensional heat conduction through a volume element in a large plane wall. Retrieved from [23].

But we know that the change in the energy and the rate of heat generation within the element can be expressed as:

$$\Delta E_{element} = mC(T_{t+\Delta t} - T_t) = \rho C A \Delta x (T_{t+\Delta t} - T_t) \qquad (1.10)$$

$$G_{element} = \dot{g} V_{element} = \dot{g} A \Delta x \qquad (1.11)$$

Substituting into Eq: 1.9, we get:

$$\dot{Q}_x - \dot{Q}_{x+\Delta x} + \dot{g} A \Delta x = \rho C A \Delta x \frac{T_{t+\Delta t} - T_t}{\Delta t} \qquad (1.12)$$

Dividing by AΔx gives:

$$-\frac{1}{A}\frac{\dot{Q}_{x+\Delta x} - \dot{Q}_x}{\Delta x} + \dot{g} = \rho C \frac{T_{t+\Delta t} - T_t}{\Delta t} \qquad (1.13)$$

Taking the limit as Δx$\to$0 and Δt$\to$0:

$$\frac{\partial}{\partial x}\left(k\frac{\partial T}{\partial x}\right) + \dot{g} = \rho C \frac{\partial T}{\partial t} \qquad (1.14)$$

This is the equation of one dimensional heat conductivity Eq: 1.14
Most heat transfer problems encountered in practice can be approximated as being one dimensional. However, this is not always the case, and we need to consider heat transfer in other directions as well. In such cases heat conduction is said to be multidimensional.

General heat conduction equation

Now, we consider a small rectangular element of length x, width y, and height z and we follow exactly the same steps with the one dimensional heat conduction equation. As a result, we end up with the general heat conduction equation for rectangular coordinates:

$$\frac{\partial}{\partial x}\left(k\frac{\partial T}{\partial x}\right) + \frac{\partial}{\partial y}\left(k\frac{\partial T}{\partial y}\right) + \frac{\partial}{\partial z}\left(k\frac{\partial T}{\partial z}\right) + \dot{g} = \rho C \frac{\partial T}{\partial t} \qquad (1.15)$$

1.1.6   Boundary and initial conditions

The heat conduction equations that we saw earlier, were developed using an energy balance on a differential element inside a medium, and they remain the same regardless of the thermal conditions on the surfaces of the medium. That is, the differential equations do not incorporate any information related to the conditions on the surfaces such as the surface temperature or a specified heat flux. However, the description of a heat transfer problem in a medium is not complete without a full description of the thermal conditions at the bounding surfaces of the medium, since we know that the heat flux and the temperature distribution in a medium depend on the conditions at the surfaces. The mathematical expressions of the thermal conditions at the boundaries are called the boundary conditions. Boundary conditions most commonly encountered in practice are the specified temperature, specified heat flux, convection, and radiation boundary conditions.

Similarly, it is also important to know at a specified time, at any point of the medium, the temperature, in order to fully describe the heat transfer problem. Such a condition, which is usually specified at time t=0, is called the initial condition, which is mathematical expression for the temperature distribution of the medium initially.

1.2   Continuum mechanics

Continuum mechanics is a branch of mechanics that deals with the mechanical behavior of materials modeled as a continuous mass rather than as discrete particles. It is known that every physical object is made up of molecules, atoms and even smaller particles. These particles are not continuously distributed over the object. However, on length scales much greater than that of inter-atomic distances, models that assume an object as a continuum, are highly accurate and useful for common engineering applications. Most of the relationships that follows based on the [12, 13, 14, 15][2].

1.2.1   Kinematics of deformation

The position of all the material points at a particular time defines the so called configuration of the body. Therefore, the configuration of a body is identified with a region in a three dimensional Euclidean space relative to an observer. In order to describe the motion and deformation of a material body the concept of frame of reference is needed since it is an observer who captures the motion. It is convenient to choose a particular configuration as a reference and to identify that frame as the reference configuration of the material body, that usually this is the body position at time equal to zero or the undeformed configuration. A current configuration is considered to be the body position at the current time or the deformed configuration.

In a mathematical way we could say the following. Let $\mathcal{B}$ denote an abstract body and $\mathcal{P} \in \mathcal{B}$ a typical material particle belonging to the body. Furthermore, let $K_r(B)$ and $K_t(B)$ denote the reference and current placements of the body in Euclidean space, respectively. Here K_r and K_t are one-to-one mappings from $\mathcal{B}$ into the reference and current placements. Let $\mathbf{X}$ denote the typical position vector of a material particle in the reference configuration $K_r(B)$ of the body, and let $\mathbf{x}$ denote the corresponding position vector of the same particle in the deformed configuration $K_t(B)$ at time t. The coordinates $\mathbf{x}$ of the so called current configuration are denoted as spatial coordinates, and assign to material points $\mathbf{X}$ places in space at a particular time. It is clear then that motion means that material particles change their

---

[2]Large portion of this chapter is also based on lecture notes from the Continuum Mechanics class of Prof. N. Aravas, especially for the section of Plasticity. Responsibility for any errors solely concerns the author.

locations in time. Thus, we can express the motion of the body as:

$$\mathbf{x} = \boldsymbol{\chi}(\mathbf{X}, t) \tag{1.16}$$

The Eq: 1.16 can be rewritten as:

$$\mathbf{x} = \mathbf{X} + \mathbf{u} \tag{1.17}$$

where $\mathbf{u}$ is the displacement field:

$$\mathbf{u} = \mathbf{x} + \mathbf{X} <=> \mathbf{u}(\mathbf{X}, t) = \mathbf{x}(\mathbf{X}, t) - \mathbf{X} \tag{1.18}$$
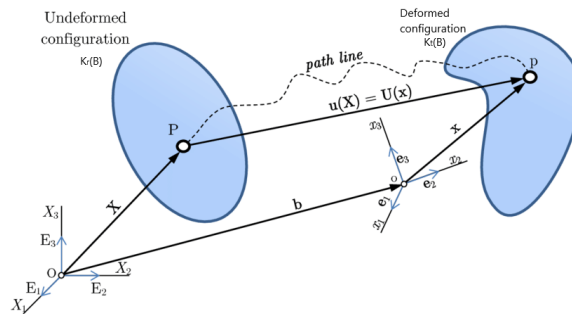
Figure (1.2)   Motion of a continuum body. Retrieved from [24].

Deformation analysis

Consider two stationary configurations, an initial and a current one, and analyze the deformation of the body that occurs between these two configurations. This is described by the deformation map $\boldsymbol{\chi}$ which takes points $\mathbf{X}$ in the initial configuration to points $\mathbf{x}$ in the current configuration[3]. The first concept to be introduced is the deformation gradient tensor, which is a measure of the local deformation of the body. Consider two very close points

---

[3]Note here that the deformation of a body must satisfy two conditions. First, any two different points from the initial configuration cannot occupy the same position in the current configuration. Second, matter cannot trespass itself. Mathematically this is guaranteed by imposing that the deformation mapping $\boldsymbol{\chi}$ is a bijection mapping (one-to-one and onto) between the two configurations under consideration.

in the initial configuration given by the relative differential $d\mathbf{X}=\mathbf{X}_1 - \mathbf{X}_0$. In the current configuration under the mapping $\boldsymbol{\chi}$ the relative position of points $\mathbf{X}_1$ and $\mathbf{X}_0$ is given by the vector $d\mathbf{x}$. Since the mapping function $\mathbf{x} = \boldsymbol{\chi}(\mathbf{X},t)$ is considered to be continuous, it follows that $d\mathbf{x}=\mathbf{F}d\mathbf{X}$, where $\mathbf{F}$ is called the deformation gradient tensor[4] and described as:

$$\mathbf{F} = \vec{\nabla}_\mathbf{x}\boldsymbol{\chi} = \frac{\partial\boldsymbol{\chi}(\mathbf{X},t)}{\partial\mathbf{X}} \tag{1.19}$$

or

$$F_{ij}(\mathbf{X},t) = \frac{\partial x_i(\mathbf{X},t)}{\partial X_j} \tag{1.20}$$

So:

$$d\mathbf{x} = \mathbf{F}d\mathbf{X} = \begin{bmatrix} \partial x_1/\partial X_1 & \partial x_1/\partial X_2 & \partial x_1/\partial X_3 \\ \partial x_2/\partial X_1 & \partial x_2/\partial X_2 & \partial x_2/\partial X_3 \\ \partial x_3/\partial X_1 & \partial x_3/\partial X_2 & \partial x_3/\partial X_3 \end{bmatrix} \begin{bmatrix} dX_1 \\ dX_2 \\ dX3 \end{bmatrix} \tag{1.21}$$

Consider a surface S_r in B_r which deforms into the surface S_t. Let $\mathbf{X}$ be a point on S_r and $\mathbf{x}$ the corresponding point on S_t. Let $d\mathbf{X}$ and $d\mathbf{X}'$ be the sides of a parallelogram on S_r based at $\mathbf{X}$. The surface area of the parallelogram is $d\mathrm{A}$, and $\boldsymbol{N}$ is the parallelogram unit normal at $\mathbf{X}$. After the deformation, based at $\mathbf{x}=\boldsymbol{\chi}(\mathbf{X},t)$, the deformed parallelogram has sides $d\mathbf{x}=\mathbf{F}d\mathbf{X}$ and $d\mathbf{x}'=\mathbf{F}d\mathbf{X}'$, the surface area is $d\mathrm{a}$ and the unit normal is $\mathbf{n}$. For the undeformed parallelogram, $\mathbf{N}d\mathrm{A}=d\mathbf{X}\times d\mathbf{X}'$. For the deformed parallelogram:

$$\mathbf{n}da = d\mathbf{x} \times d\mathbf{x}' = [(\mathbf{F}d\mathbf{X}) \times (\mathbf{F}d\mathbf{X}')] = J\mathbf{F}^{-T}(d\mathbf{X} \times d\mathbf{X}') \tag{1.22}$$

So we get:

$$\mathbf{n}da = J\mathbf{F}^{-T}(d\mathbf{X} \times d\mathbf{X}') = JdA\mathbf{F}^{-T}\mathbf{N} \tag{1.23}$$

---

[4]If the deformation gradient is constant, i.e. it is the same for every material point $\mathbf{X}$, then the deformation is said to be homogeneous. On the other hand, the deformation is said to be non homogeneous if $\mathbf{F}$ is a function of the material point $\mathbf{X}$

This important result, known as Nanson's formula [5] describes how elements of surface area deform.

Now we consider an undeformed volume element dV in the body consisting of a parallelepiped with sides $d\boldsymbol{X}_1$, $d\boldsymbol{X}_2$, $d\boldsymbol{X}_3$ so that $dV = (d\boldsymbol{X}_2 \times d\boldsymbol{X}_3) \cdot d\boldsymbol{X}_1$. After deformation this volume becomes $dv = (d\boldsymbol{x}_2 \times d\boldsymbol{x}_3) \cdot d\boldsymbol{x}_1$, where the $d\boldsymbol{x}_1$, $d\boldsymbol{x}_2$, and $d\boldsymbol{x}_3$ represent the vectors forming the sides of the deformed volume.

So:

$$dv = (\mathbf{F}\, d\boldsymbol{X}_2 \times \mathbf{F}\, d\boldsymbol{X}_3) \cdot \mathbf{F}\, d\boldsymbol{X}_1 = \det(\mathbf{F})\, dV = J\, dV \tag{1.24}$$

Therefore:

$$dv = J\, dV \tag{1.25}$$

Stretch and shear are deformation measures related to the deformation gradient. Stretch is defined, for instance, at a material point $\mathbf{X}$ in a particular direction as the ratio of the deformed length to the initial length in that particular undeformed direction. On the other hand, the change between an angle in the initial configuration and its corresponding value in the current configuration is called shear. Different measures of deformation are used apart from the deformation gradient tensor, that is a local measure of the deformation. The reason is to impart physical meaning to the measurement of deformation, such as change of lengths and orientations in particular directions. This kind of measurement is usually denoted as strain. Strain is also measured locally and accounts for changes in different geometrical quantities.

Material Strain Tensors

The change in the length of a line element ds_0 is given by:

$$ds = \sqrt{d\mathbf{x} \cdot d\mathbf{x}} \tag{1.26}$$

---

[5]https://en.wikiversity.org/wiki/Continuum_mechanics/Volume_change_and_area_change

by using Eq: 1.21, Eq: 1.26 can be rewritten as:

$$ds = \sqrt{(d\mathbf{X}\mathbf{F}^T) \cdot (\mathbf{F}\,d\mathbf{X})} = \sqrt{d\mathbf{X} \cdot \mathbf{C}\,d\mathbf{X}}, \quad \mathbf{C} = \mathbf{F}^T\mathbf{F} \tag{1.27}$$

where $\mathbf{C}$ is known as the right Cauchy-Green deformation tensor.
In Cartesian component form Eq: 1.26 can be written as:

$$ds = \sqrt{\frac{\partial x_i}{\partial X_j}\frac{\partial x_i}{\partial X_k}\partial X_j \partial X_k} \tag{1.28}$$

Eq: 1.28 can be written in component form in terms of the material description of the displacement $\mathbf{u}(\mathbf{X}, t) = \mathbf{x}(\mathbf{X}, t) - \mathbf{X}$ by substituting with: $\frac{\partial x_i}{\partial X_k} = \delta_{ik} + \frac{\partial u_i}{\partial X_k}$ and $\frac{\partial x_i}{\partial X_j} = \delta_{ij} + \frac{\partial u_i}{\partial X_j}$, so:

$$ds = \sqrt{(\delta_{jk} + 2E_{jk})\partial X_j \partial X_k} \tag{1.29}$$

where E_{jk} defined as:

$$E_{jk} = \frac{1}{2}\left(\frac{\partial u_j}{\partial X_k} + \frac{\partial u_k}{\partial X_j} + \frac{\partial u_i}{\partial X_j}\frac{\partial u_i}{\partial X_k}\right) \tag{1.30}$$

and is called the Green-Lagrange strain tensor.

Infinitesimal Deformations

When displacement gradients are small: $\frac{\partial u_i}{\partial X_j} << 1$, their products can be neglected from Eq: 1.30:

$$E_{jk} = \frac{1}{2}\left(\frac{\partial u_j}{\partial X_k} + \frac{\partial u_k}{\partial X_j}\right) <=> \varepsilon_{ij} = \frac{1}{2}\left(\frac{\partial u_i}{\partial X_j} + \frac{\partial u_j}{\partial X_i}\right) \tag{1.31}$$

It is clear that when the displacement $\mathbf{u}$ is known, the strain tensor $\boldsymbol{\varepsilon}$ follows from Eq: 1.31. Nevertheless, in many elasticity problems the three components of the displacement are unknown, and furthermore these have to be calculated from the six components of the strain tensor $\boldsymbol{\varepsilon}$. This suggests that the six independent components of the strain tensor must be related. These

relations are known as the equations of compatibility, which can be written in terms of symmetric incompatibility tensor **S**, which is given by:

$$S_{ij} = -e_{ipm}e_{jqn}\varepsilon_{pq,mn} = 0 \tag{1.32}$$

where $e_i = \varepsilon_i - \frac{\varepsilon_{kk}}{3}$
Eq: 1.32 yields 81 equations, that are known as the compatibility equations, which only six of them are not identically zero.

1.2.2 Stresses and balance equations

The mechanics of continuous media are described by equations which express the balance of mass, linear momentum, angular momentum and energy in a moving body. These balance equations must be obeyed by all moving bodies and each one gives rise to field equations for sufficiently smooth motions.

Mass and conservation of mass

Clearly mass is a positive quantity as well as the mass density. It is possible to designate a mass element $dm(\mathbf{X}) = \rho_o(\mathbf{X})dV$. So, the total mass M of the body is:

$$M = \int_B dm(\mathbf{X})dV = \int_B \rho_o(\mathbf{X})dV = \int_{B_t} \rho(\mathbf{x},t)dv \tag{1.33}$$

where $\rho(\mathbf{x},t)$ represents mass density in the current configuration. The total mass M of the body before (B) and after deformation (B_t) does not change, so:

$$\frac{dM}{dt} = \frac{d}{dt}\int_{B_t} \rho(\mathbf{x},t)dv = \int_{B_t} \frac{\partial\rho(\mathbf{x},t)}{\partial t}dv + \int_{\partial B_t} \rho(\mathbf{x},t)\mathbf{v}(\mathbf{x},t)\cdot\mathbf{n}ds = 0 \tag{1.34}$$

By using the divergence theorem, we can obtain the continuity equation, which is a form of the conversation of mass:

$$\int_{B_t} \left(\frac{\partial \rho(\mathbf{x},t)}{\partial t} + div(\rho(\mathbf{x},t)\mathbf{v}) \right) dv = 0 <=> \frac{\partial \rho(\mathbf{x},t)}{\partial t} + div(\rho(\mathbf{x},t)\mathbf{v}) = 0$$

$$(1.35)$$

Stress analysis

The manner in which the surroundings of a body act over the body as well as the way some parts of a body act over other parts of the body are described by means of forces and torques. Forces (torques) are classified as body forces (body torques) or contact forces (contact torques) also known as surface forces (surface torques). Body forces that act on the volume (or mass) of the body has its origin outside of the body. Surface forces can be either external to the body when acting on the boundary of the body, or internal to the body when acting between different parts within the body. Stress measures the internal contact forces per unit area acting between particles of the body across internal surfaces. The mathematical description of surface forces is based on Cauchy's principal, which can be stated as follows: upon any closed surface S (real or imaginary) that divides the body in two parts, the action of one part of the body on the other is represented by a vector field $\boldsymbol{t^n}$ called the stress vector, defined on the surface S with physical dimensions of force per unit area and assumed to depend continuously on the surface unit vector $\mathbf{n}$.

At a point in the deformed configuration of the body, consider a small surface element of area ΔA having unit normal $\mathbf{n}$ on which a force ΔF acts. Then $\mathbf{t^n}$ = $\lim_{\Delta A \to 0}(\Delta \mathbf{F}/\Delta A)$ is the stress vector acting at this point. Cauchy conjectured the existence of a stress tensor $\boldsymbol{\sigma}$ which, when acting on the surface normal $\mathbf{n}$ at a point in the deformed body, yielded the stress vector at that point. This is known as Cauchy's stress theorem and basically it is based on the fact that by knowing the stress vectors on three mutually perpendicular planes, the traction vector $\mathbf{t^n}$ on any other plane passing through that point can be found. That is:

$$\mathbf{t^n} = \boldsymbol{\sigma}\mathbf{n} \tag{1.36}$$

The Cauchy stress tensor refers to forces per unit area of the deformed con-

figuration. Based on Eq: 1.36 the components of $\boldsymbol{\sigma}$ ($\boldsymbol{\sigma} = \sigma_{ij}\mathbf{e}_i \otimes \mathbf{e}_j$) in a Cartesian coordinate system with base vectors $(\mathbf{e}_1, \mathbf{e}_2, \mathbf{e}_3)$ are computed as: $\sigma_{ij} = \mathbf{e}_i \cdot \boldsymbol{\sigma}\mathbf{e}_j$, where $\boldsymbol{\sigma}\mathbf{e}_j$ is simply the stress vector acting on a plane whose normal is the $\mathbf{e}_j$ direction.

Euler's Law of Motion

The motion of a material body produced by the action of surface forces and body forces. When surface and body forces act upon a body, surface or contact forces are transmitted from point to point inside the body according to Euler's laws of motion: conservation of linear momentum and conservation of angular momentum.

Conservation of Linear Momentum

Principle of linear momentum states that the time rate of change of this momentum is equal to the net force acting on the mass. The concept is extended to a continuum body by considering the linear momentum of the entire mass, so that denoting the force by $\boldsymbol{F}$, the balance of linear momentum is written as:

$$\dot{\boldsymbol{\mathcal{L}}} = \frac{d}{dt}\int_{B_t} \rho(\mathbf{x}, t)\mathbf{v}(\mathbf{x}, t)\, dv = \boldsymbol{F} \tag{1.37}$$

The resultant $\boldsymbol{F}$ consists in general of a body force term and surface forces. If $\boldsymbol{\beta}$ denotes the body force per unit mass and $\mathbf{t}$ the stress vector, then: $\boldsymbol{F} = \int_{B_t} \rho\boldsymbol{\beta}\, dv + \int_{S_t} \mathbf{t}\, ds$. Therefore the conservation of linear momentum Eq: 1.37 takes the form:

$$\int_{B_t} \rho(\mathbf{x}, t)\frac{d}{dt}(\mathbf{v}(\mathbf{x}, t))\, dv = \int_{B_t} \rho\boldsymbol{\beta}\, dv + \int_{S_t} \mathbf{t}\, ds \tag{1.38}$$

$$\int_{B_t} \rho(\mathbf{x}, t)\dot{\mathbf{v}}(\mathbf{x}, t)\, dv = \int_{B_t} (\rho\boldsymbol{\beta} + div\boldsymbol{\sigma})\, dv \tag{1.39}$$

Consequently, one can write the local form of Eq: 1.39 known as the Eulerian equations of motion as:

$$\boldsymbol{\nabla}\boldsymbol{\sigma} + \rho\boldsymbol{\beta} = \rho\dot{\mathbf{v}}(\mathbf{x}, t) \tag{1.40}$$

$$\boldsymbol{\nabla}\boldsymbol{\sigma} + \rho\boldsymbol{\beta} = \rho\mathbf{a}(\mathbf{x}, t) \tag{1.41}$$

where $\mathbf{a}(\mathbf{x}, t)$ is the acceleration of the body. In case of zero acceleration, the latter reduces to the **equilibrium equations**:

$$\boldsymbol{\nabla}\boldsymbol{\sigma} + \rho\boldsymbol{\beta} = 0 \tag{1.42}$$

$$\frac{\partial \sigma_{ji}}{\partial X_j} + \rho\beta_i = 0, \qquad i = 1, 2, 3 \tag{1.43}$$

Conservation of Angular Momentum

The rate of change of the angular momentum is equal to the resultant moment acting on the mass. The angular momentum of the body is given by:
$\mathcal{H} = \int_{B_t} \mathbf{r} \times [\rho(\mathbf{x}, t)\mathbf{v}(\mathbf{x}, t)]\, dv$.
Thus:

$$\frac{d}{dt}\mathcal{H} = \int_{B_t} (\mathbf{r} \times \rho\boldsymbol{\beta})\, dv + \int_{S_t} (\mathbf{r} \times \mathbf{t})\, ds \tag{1.44}$$

In component form:

$$\int_{B_t} \varepsilon_{ijk} x_j \rho\dot{v}_k\, dv = \int_{B_t} \rho\varepsilon_{ijk} x_j \beta_k\, dv + \int_{S_t} \varepsilon_{ijk} x_j \sigma_{kp} n_p\, ds \tag{1.45}$$

$$\int_{B_t} \varepsilon_{ijk} x_j \rho\dot{v}_k\, dv = \int_{B_t} \rho\varepsilon_{ijk} x_j \beta_k\, dv + \int_{B_t} \varepsilon_{ijk}\left(x_j \frac{\partial}{\partial x_p}\sigma_{kp} + \sigma_{kj}\right) dv \tag{1.46}$$

$$\int_{B_t} \varepsilon_{ijk} x_j \left[-\rho\dot{v}_k + \rho\beta_k + \frac{\partial}{\partial x_p}\sigma_{kp}\right] dv + \int_{B_t} \varepsilon_{ijk} \sigma_{kj}\, dv = 0 \tag{1.47}$$

where $-\rho\dot{v}_k + \rho\beta_k + \frac{\partial}{\partial x_p}\sigma_{kp}$ is the linear momentum equation so it is identically zero. Hence, $\varepsilon_{ijk}\sigma_{kj} = 0$, which signifies that $\sigma_{kj} = \sigma_{jk}$, or that $\boldsymbol{\sigma}$ is

symmetric:

$$\boldsymbol{\sigma} = \boldsymbol{\sigma}^T \tag{1.48}$$

1.2.3   Elastic deformation

In order to solve a mechanical problem, the following groups of equations are required:

1. Equilibrium equations.
2. Equations of compatibility of deformation.
3. Constitutive equations of forces and displacements.

In sections 1.2.1 and 1.2.2 the equations of compatibility of deformations and equilibrium equations were presented. The equations that connect stresses and deformations are called constitutive equations and they depend on the properties of the material.

In general, each component of stress tensor σ_{ij} in a material point depends on all the components of infinitesimal deformation tensor ε_{ij}, the temperature T, the history of deformation and some other factors, such as porosity, moisture etc.

In most applications it is assumed that the behavior at a point is only affected by what has happened only in a small neighborhood of the point under study. This postulate, known as local constitutive theory, gives rise to the so called simple materials. That means that each component of stress tensor σ_{ij} in a material point depends on the components of infinitesimal deformation tensor ε_{ij}, the temperature T etc, at the same material point, and it does not being affected by the values of $\boldsymbol{\varepsilon}$, T etc at the rest of the body.

Furthermore, for linearly elastic materials the relation between the components of stress tensor σ_{ij} and the components of infinitesimal deformation tensor ε_{ij} is linear. A solid behaves like a linear elastic material when it returns to its original unloaded state, upon removal of the loading. Of course this behavior applies, as much as the stresses are below a certain limit, which is different for each material.

In a simple elastic material, where the stress tensor $\boldsymbol{\sigma}$ in a material point

X depends only on infinitesimal deformation tensor in that material point, then the general form of the constitutive equation is:

$$\boldsymbol{\sigma}(\mathbf{X}) = \mathbf{f}(\boldsymbol{\varepsilon}(\mathbf{X}), \mathbf{X}) \tag{1.49}$$

where **f** is a second order tensile function. If the mechanical properties are the same in all of the material points, then the material defines as homogeneous and so **f** does not depend on **X** and the constitutive equation turns to:

$$\boldsymbol{\sigma}(\mathbf{X}) = \mathbf{f}(\boldsymbol{\varepsilon}(\mathbf{X})) = \mathbf{f}(\boldsymbol{\varepsilon}) \tag{1.50}$$

So, in the case of linearly elastic materials, **f** is a linear function of $\boldsymbol{\varepsilon}$. That means that each component of the stress tensor σ_{ij} in a material point is linear related to the components of infinitesimal deformation tensor ε_{ij} and the general form of the constitutive equation is:

$$\sigma_{ij} = \mathcal{L}_{ijkl}\varepsilon_{kl} \tag{1.51}$$

There are 81 physical constants $\mathcal{L}$, which express properties of the material in the directions of the axes of the system, in which σ_{ij} and ε_{ij} are being computed. These constants are called elastic constants and they are independent of the deformation.
In tensile form the constitutive equation is expressed as:

$$\boldsymbol{\sigma} = \boldsymbol{\mathcal{L}} : \boldsymbol{\varepsilon} \tag{1.52}$$

Where $\boldsymbol{\mathcal{L}}$ are a fourth order tensor and is called elasticity tensor. Furthermore, The stress and strain tensor are symmetric and they define 6 independent linear equations, so $\boldsymbol{\mathcal{L}}$ also is symmetric.

$$\mathcal{L}_{ijkl} = \mathcal{L}_{jikl} = \mathcal{L}_{ijlk} \tag{1.53}$$

For isotropic linearly elastic material:

$$\boldsymbol{\mathcal{L}} = 2G\boldsymbol{\mathcal{K}} + 3\kappa\boldsymbol{\mathcal{J}} \tag{1.54}$$

$$\mathcal{K}_{ijkl} = \mathcal{I}_i jkl - \mathcal{J}_{ijkl} \tag{1.55}$$

$$\mathcal{I}_{ijkl} = \frac{1}{2}(\delta_{ik}\delta_{jl} + \delta_{il}\delta_{jk}) \tag{1.56}$$

$$\mathcal{J}_{ijkl} = \frac{1}{3}\delta_{ij}\delta_{kl} \tag{1.57}$$

$$G = \frac{E}{2(1+v)} \tag{1.58}$$

$$\kappa = \frac{E}{3(1-2v)} \tag{1.59}$$

where G is the elastic shear modulus, κ is the elastic expansion modulus and v is the Poisson's ratio.

In a continuous body, a deformation field results from a stress field induced by applied forces or is due to changes in the temperature field inside the body. Temperature differences (ΔT) of an infinitesimal isotropic elastic element, leads to its uniform expansion in all directions. That means there will be equal normal strains in all directions and no shear strains. Thus, the infinitesimal thermal expansion of infinitesimal material fiber is calculated from the following equation:

$$\varepsilon^{thermal} = \alpha\Delta T \tag{1.60}$$

In this case, the components of the tensor of the infinitesimal thermal deformation are:

$$\varepsilon_{ij}^{thermal} = \alpha\Delta T\delta_{ij} \tag{1.61}$$

where $\delta_{ij} = \begin{cases} 0 & \text{if } i \neq j \\ 1 & \text{if } i = j \end{cases}$ is the Kronecker delta and α is the thermal expansion coefficient.

So in general, the components of the total infinitesimal deformation tensor, when mechanical and thermal loads are applied to an infinitesimal isotropic material element, are calculated from the following equations:

$$\varepsilon_{11} = \frac{1}{E}[\sigma_{11} - v(\sigma_{22} + \sigma_{33})] + \alpha\Delta T \tag{1.62}$$

$$\varepsilon_{22} = \frac{1}{E}[\sigma_{22} - v(\sigma_{33} + \sigma_{11})] + \alpha\Delta T \tag{1.63}$$

$$\varepsilon_{33} = \frac{1}{E}[\sigma_{33} - v(\sigma_{11} + \sigma_{22})] + \alpha\Delta T \tag{1.64}$$

$$\varepsilon_{12} = \frac{\sigma_{12}}{2G} \tag{1.65}$$

$$\varepsilon_{13} = \frac{\sigma_{13}}{2G} \tag{1.66}$$

$$\varepsilon_{23} = \frac{\sigma_{23}}{2G} \tag{1.67}$$

1.2.4 The boundary value problem

In order to determine the displacements, the deformations and the stresses on a linearly elastic body, it takes to combine the equilibrium equations, the equations of compatibility of deformation and the constitutive equations with the appropriate boundary conditions, forming the boundary value problem. Assuming a body with reference configuration $\mathcal{B}$, the boundary conditions on $\partial\mathcal{B}$ are:

$$\mathbf{u} = \hat{\boldsymbol{u}} \quad on \quad \partial\mathcal{B}_u \tag{1.68}$$

$$\boldsymbol{\sigma} \cdot \mathbf{n} = \hat{\boldsymbol{t}} \quad on \quad \partial\mathcal{B}_t \tag{1.69}$$

$$\mathbf{u} \cdot \mathbf{n} = \hat{u}_n \quad and \quad \boldsymbol{\sigma} \cdot \mathbf{n} - (\mathbf{n} \cdot \boldsymbol{\sigma} \cdot \mathbf{n})\mathbf{n} = \hat{\boldsymbol{t}}^s \quad on \quad \partial\mathcal{B}_{ut1} \tag{1.70}$$

$$\mathbf{n} \cdot \boldsymbol{\sigma} \cdot \mathbf{n} = \hat{t}_n \quad and \quad \mathbf{u} - (\mathbf{u} \cdot \mathbf{n})\mathbf{n} = \hat{\boldsymbol{u}}_{\boldsymbol{s}} \quad on \quad \partial\mathcal{B}_{ut2} \tag{1.71}$$

where $\mathbf{n}$ represents the positive (outward) unit normal to the boundary $\partial\mathcal{B}$, $\hat{\boldsymbol{u}}$ represents the applied displacements on the section $\partial\mathcal{B}_u$ of $\partial\mathcal{B}$ and $\hat{\boldsymbol{t}}$ represents the applied surface forces to the rest $\partial\mathcal{B}_t$ of $\partial\mathcal{B}$ ($\partial\mathcal{B}_u \cup \partial\mathcal{B}_t = \partial\mathcal{B}$ and $\partial\mathcal{B}_u \cap \partial\mathcal{B}_t = \varnothing$). There is also a section of the boundary where it is applied the part of the $\mathbf{u}$ (or $\boldsymbol{\sigma} \cdot \mathbf{n}$) which is normal to $\partial\mathcal{B}$ and a part of $\boldsymbol{\sigma} \cdot \mathbf{n}$ (or $\mathbf{u}$) which is tangential to $\partial\mathcal{B}$. In this case: $\partial\mathcal{B}_u \cup \partial\mathcal{B}_t \cup \partial\mathcal{B}_{ut} = \partial\mathcal{B}$ and

$\partial\mathcal{B}_u \cap \partial\mathcal{B}_t = \partial\mathcal{B}_u \cap \partial\mathcal{B}_{ut} = \partial\mathcal{B}_t \cap \partial\mathcal{B}_{ut} = \varnothing$.

Furthermore, it is assumed that the applied loads on the elastic body are changing with really slow rates and the body is in constantly condition of pseudo equilibrium, which is a linear elastostatic problem. So, to recapitulate, the boundary value problem can be expressed as:

$$\nabla\boldsymbol{\sigma} + \rho\boldsymbol{\beta} = 0 \tag{1.72}$$

$$\boldsymbol{\varepsilon} = \frac{1}{2}(\mathbf{u}\nabla + \nabla\mathbf{u}) \tag{1.73}$$

$$\boldsymbol{\mathcal{L}} = 2G\boldsymbol{\mathcal{K}} + 3\kappa\boldsymbol{\mathcal{J}} \tag{1.74}$$

$$\mathbf{u} = \hat{\boldsymbol{u}} \quad on \quad \partial\mathcal{B}_u \tag{1.75}$$

$$\boldsymbol{\sigma}\cdot\mathbf{n} = \hat{\boldsymbol{t}} \quad on \quad \partial\mathcal{B}_t \tag{1.76}$$

$$\mathbf{u}\cdot\mathbf{n} = \hat{u}_n \quad and \quad \boldsymbol{\sigma}\cdot\mathbf{n} - (\mathbf{n}\cdot\boldsymbol{\sigma}\cdot\mathbf{n})\mathbf{n} = \hat{\boldsymbol{t}}^s \quad on \quad \partial\mathcal{B}_{ut1} \tag{1.77}$$

$$\mathbf{n}\cdot\boldsymbol{\sigma}\cdot\mathbf{n} = \hat{t}_n \quad and \quad \mathbf{u} - (\mathbf{u}\cdot\mathbf{n})\mathbf{n} = \hat{\boldsymbol{u}}_{\boldsymbol{s}} \quad on \quad \partial\mathcal{B}_{ut2} \tag{1.78}$$

1.2.5 Plasticity

In physics and materials science, plasticity, also known as plastic deformation, is the ability of a solid material to undergo permanent deformation, a non-reversible change of shape in response to applied forces.

In plastic deformation the problem is described by the same equations as in elastic deformation, except from the constitutive equations, where here the relation between stress and strain can not be linear. This is obvious as a certain stress can correspond to multiple strains. In order to implement the appropriate relation between stress and strain in plasticity, it is important to determine if the material point under consideration is in the elastic or plastic region, using a yield function and then it is important to determine if this point continuous to deform plastically or if it unloads elastically, using an elastic predictor.

The yield function Φ can be expressed as:

$$\Phi(\boldsymbol{\sigma}, q_a) = 0, \qquad a = 1, 2, ..., n \tag{1.79}$$

$$\dot{q}_a = \dot{\lambda}g_a(\boldsymbol{\sigma}, q_\beta) \tag{1.80}$$

where q_a [6] are constitutive variables, which are changing as the plastic deformation occurs and depend on the material, such as the yield point of the material, which increases as the plastic deformation takes place.
The plastic deformation rate is described as:

$$\dot{\varepsilon}^P = \dot{\lambda} \mathbf{N} \tag{1.81}$$

$$\mathbf{N} = \frac{\partial \Phi}{\partial \boldsymbol{\sigma}} \tag{1.82}$$

$$\dot{\lambda} = \begin{cases} \frac{1}{H} \mathbf{N} : \dot{\boldsymbol{\sigma}} & \text{if } H \neq 0, \quad \dot{\boldsymbol{\sigma}} : known \\ \frac{1}{L} \mathbf{N} : \boldsymbol{\mathcal{L}}^e : \dot{\boldsymbol{\varepsilon}} & \text{if } \dot{\boldsymbol{\varepsilon}} : known \end{cases} \tag{1.83}$$

$$H = -\sum_{a=1}^{n} \frac{\partial \Phi}{\partial q_a} g_a \tag{1.84}$$

$$L = H + \mathbf{N} : \boldsymbol{\mathcal{L}}^e : \mathbf{N} \tag{1.85}$$

For von Mises yield criterion, the yield function is described as:

$$\Phi(\boldsymbol{\sigma}, \bar{\varepsilon}^P) = \sigma_e(\boldsymbol{\sigma}) - \sigma_Y(\bar{\varepsilon}^P) = 0 \tag{1.86}$$

$$\sigma_e = \sqrt{\frac{3}{2} s_{ij} s_{ij}} \tag{1.87}$$

$$g_1 = 1 \tag{1.88}$$

$$q_1 = \bar{\varepsilon}^P \tag{1.89}$$

$$\dot{\lambda} = \dot{\bar{\varepsilon}}^P \tag{1.90}$$

$$\dot{\varepsilon}^P = \dot{\bar{\varepsilon}}^P \mathbf{N} \tag{1.91}$$

$$\mathbf{N} = \frac{3}{2\sigma_e} \mathbf{s} \tag{1.92}$$

where $\mathbf{s}$ is the stress deviator tensor, $\bar{\varepsilon}^P$ is the equivalent plastic strain, σ_e is the equivalent von Mises stress and σ_Y is the yield strength that indicates the beginning of plastic deformation.

---

[6]It is assumed, that it is rate independent, which means is independent of time. Usually this is true for solids.

As mentioned earlier, it is important when the material point is in the plastic region, to determine whether it continuous to deform plastically or it unloads elastically, in order to implement the appropriate relation between stress and strain and to achieve it, the elastic predictor is used.

In general, in the plastic region the relation between stress and strain is: $\dot{\boldsymbol{\sigma}} = \boldsymbol{\mathcal{L}} : \dot{\boldsymbol{\varepsilon}}$ and $\boldsymbol{\mathcal{L}}$ is defined as:

$$\boldsymbol{\mathcal{L}} = \begin{cases} \boldsymbol{\mathcal{L}}^e & \text{if } \boldsymbol{N} : \boldsymbol{\mathcal{L}}^e : \dot{\boldsymbol{\varepsilon}} \leqslant 0 \\ \boldsymbol{\mathcal{L}}^{ep} & \text{if } \boldsymbol{N} : \boldsymbol{\mathcal{L}}^e : \dot{\boldsymbol{\varepsilon}} > 0 \end{cases} \tag{1.93}$$

$$\boldsymbol{\mathcal{L}}^e = 2G\boldsymbol{\mathcal{K}} + 3\kappa\boldsymbol{\mathcal{J}} \tag{1.94}$$

$$\boldsymbol{\mathcal{L}}^{ep} = \boldsymbol{\mathcal{L}}^e - \frac{1}{L}(\boldsymbol{\mathcal{L}}^e : \boldsymbol{N})(\boldsymbol{\mathcal{L}}^e : \boldsymbol{N}) \tag{1.95}$$

where $\boldsymbol{N} : \boldsymbol{\mathcal{L}}^e : \dot{\boldsymbol{\varepsilon}}$ is the elastic predictor, that determines which is the appropriate relationship for $\boldsymbol{\mathcal{L}}$.

Chapter 2

Description of the finite element model

2.1 Description of the model structure

In order to estimate stress and distortion in an additive manufacturing process with reasonable computational time, a 2-D finite element model was developed in ABAQUS. ABAQUS is a software suite for finite element analysis and computer-aided engineering. The most difficult part of creating this model was the need for thermomechanical coupling, because the mutual influences between displacements or strains and temperature are manifested in many different ways. This challenge has been overcome by considering the thermal analysis separately form the mechanical analysis. More specific the concept is, completing first the thermal analysis and extracting the temperature field and later applying this temperature field to the mechanical analysis, in order to estimate the thermal stresses and strains that are developing within the body.

Another challenge was, to simulate the actual process of adding material over time to the formation of the final body shape. In order to avoid complex methods of dynamic geometries, a modification of the quiet element method was used, where all the elements of the whole geometry are present since the beginning of the analysis, but they are inactive. That means, that their properties in the beginning of the analysis have values that do not allow them to interact with the active elements and so they do not affect the analysis until the laser passes over them and activates them. Here are also some other

approaches for additive manufacturing modeling [16, 17, 18, 19, 20, 21, 22].

2.2 Modified quiet element method

First of all, as it was previously mentioned we developed a 2-d model, so the laser is moving only on the x and y axis. More specific, it starts from the left side and moving horizontally along the x-axis to the right side, building a layer of material. Then is cooling off for some time while moving again on the left side, but now at a higher height along the y-axis and repeats the same process to build another layer over the previous layer.

In the quiet element method all the elements are present form the beginning of the analysis, however they are assigned properties so they do not affect the analysis. In the heat transfer analysis, the thermal conductivity k is set to a very low value to minimize conduction into the quiet elements, and the specific heat C_p respectively is set to a very low value to minimize the energy transfer to the quiet elements. But this method has the following disadvantages: If the properties of the inactive elements are not small enough, the quantities that ABAQUS computes for them may affect the analysis, resulting in errors or the Jacobian being ill-conditioned. [1]

In the modified quiet element method that it is proposed in this thesis, the properties of the inactive elements are set to zero, so it is sure that there is no way for inactive elements to affect the analysis. In order to achieve that, a user subroutine called MPC is used, that sets the displacements in all the directions to zero and the temperature equal to the initial temperature for all the inactive elements. This methodology prevents an ill-conditioned Jacobian and allows for faster computations, as it does not make calculations for the inactive elements. The MPC user subroutine in the mechanical analysis sets the displacements in all the directions for the inactive elements to zero. Respectively, the MPC user subroutine in the thermal analysis sets the temperature for the inactive elements equal to the initial temperature. Furthermore, to check if an inactive element must be set to active:

- Find position of laser beam (x^{laser}, y^{laser}).

- Calculate the local coordinates of the integration point (ξ, η)[2], where $\xi = x^{laser} - x^{npt}$ and $\eta = y^{laser} - y^{npt}$.

---

[1]an ill-conditioned problem is one where, for a small change in the inputs there is a large change in the answer or dependent variable. This means that the correct solution to the equation becomes hard to find.

[2]local coordinates at the ellipsoid center. The laser beam on the metal powder was modeled as an ellipsoid.

- check if n>tol and $|\xi| \leq \alpha$, then element is set to active, where tol=10^{-4} and α is the semi-axis of the ellipsoid in x-direction.
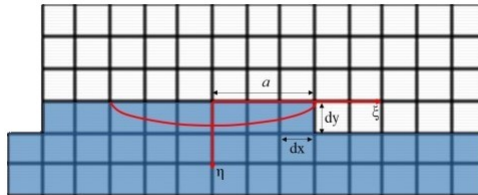

Figure (2.1)   A representation of activation of inactive elements

2.3 Thermal analysis

2.3.1 Governing equations

A well tested two dimensional heat transfer model for AM is used to compute temperature field. The model uses the energy conservation equation, that was shown in Chapter 1 Eq: 1.15

$$\boldsymbol{\nabla} \cdot (k\boldsymbol{\nabla} T) + \dot{g} = \rho C_p \frac{\partial T}{\partial t} \tag{2.1}$$

Thus for homogeneous materials:

$$k\nabla^2 T + \dot{g} = \rho C_p \frac{\partial T}{\partial t} \tag{2.2}$$

where:

- ρ [in $\frac{kg}{m^3}$] :density

- k [in $\frac{W}{m\,^\circ C}$] :conductivity

- C_p [in $\frac{J}{kg\,^\circ C}$] :specific heat

This equation is used in conjunction with the following boundary conditions:

- T=known on S_1

- $-\boldsymbol{q} \cdot \boldsymbol{n} = q_n$ =known on S_2

where q_n is the heat power flux at a point on S and it is positive when heat enters the body. In this model, it is assumed that the power flux at the boundary transfers heat only with convection and radiation, so combining the equations: 1.4 and 1.7 from Chapter 1:

$$q_n = -h(T - T_0) - \sigma\varepsilon[(T - T_z)^4 - (T_0 - T_z)^4] \tag{2.3}$$

where:

- T_0 :the room temperature

- T_z :the absolute zero temperature (T_z=-273 $^\circ$ C)

- ε :the emissivity (dimensionless)

- σ :the Stefan-Boltzmann constant (σ=5.669x10^{-8} $\frac{W}{m^2(^\circ\ C)^4}$)

- h [in $\frac{W}{m^2\ ^\circ C}$] :convection heat transfer coefficient

The heat input from the laser beam in this model is modeled as heat generation and more specific as an ellipsoid volumetric source, so the equation that simulates the heat input is:

$$\dot{g} = \frac{6P}{\pi\ a\ b\ c}e^{-3(\frac{\xi^2}{a^2}+\frac{\eta^2}{b^2})} \tag{2.4}$$

where:

- P [in W] :power of the laser

- a,b,c [in mm] are parameters of the volume of an ellipsoid

- ξ,η,ζ [in mm] are respectively local coordinates at the ellipsoid center

2.3.2 Boundary conditions implementation in ABAQUS

It is very important to apply the right boundary conditions to each element, in order to avoid any errors in the thermal analysis. The boundary conditions take into consideration both laser heating and heat losses due to convection and radiation. At first, it has to be checked whether an element is active or it has to be activated, as it was mentioned earlier. Then if the element is active or it just got activated, it has to be checked if any part of the boundary of this element, is part of the boundary of the whole body.
More specific for an element that is currently activated:

- if ($|\eta|$ <dy), then boundary conditions must be applied at the top of the element.

- for the previous element if at the same time ($|\xi|$+dx >α), then boundary conditions must be also applied at the right side of the element.

- for an element with boundary conditions at the top ($|\eta|$ <dy), if at the same time is the first element of the layer ($x^{npt} < x_0^{laser} + dx$), then boundary conditions must be applied at the left side of the element.

Furthermore, for an element that is already activated:

- if ($|\eta|$ <dy and $x^{npt} < x^{laser} + \alpha$), then boundary conditions must be applied at the top of the element.

- if ($|\eta|$ <2dy and $x^{npt} > x^{laser} + \alpha$), then boundary conditions must be applied at the top of the element.

- if ($noel > nw$ and $x^{npt} < x_0^{laser} + dx$), that means if the element belongs to the wall and it is the first element of a layer, then boundary conditions must be applied at the left side of the element. [3]

- if ($noel > nw$ and $x^{npt} > x_0^{laser} + (NUM - 1)dx$), that means if the element belongs to the wall and it is the last element of a layer, then boundary conditions must be applied at the right side of the element.
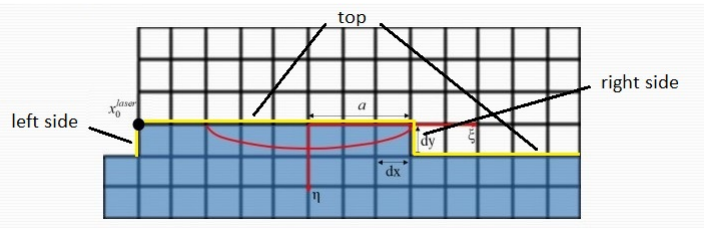
Figure (2.2)   Boundary conditions of the evolving surface

The heat source of the laser beam and the boundary conditions for convection and radiation on the evolving surface are modeled via the user subroutine DFLUX in ABAQUS.

Listing (2.1)   User subroutine interface (DFLUX)

```
1  SUBROUTINE DFLUX(FLUX,SOL,KSTEP,KINC,TIME,NOEL,NPT,COORDS,
2       1  JLTYP,TEMP,PRESS,SNAME)
3  C
4       INCLUDE 'ABA_PARAM.INC'
5  C
6       DIMENSION FLUX(2), TIME(2), COORDS(3)
7       CHARACTER*80 SNAME
8
9
10      user coding to define FLUX(1) and FLUX(2)
```

---

[3]nw=10000, the numeration of the wall elements and nodes starts from that number, in order to distinguish the wall elements from the substrate elements.

```
11
12
13          RETURN
14          END
```

where:

- FLUX(1) $\rightarrow$ Magnitude of flux flowing into the model at this point.

- FLUX(2) $\rightarrow$ Rate of change of the flux with respect to the temperature at this point.

So, as it is known, when an element is active and which boundary conditions should apply to the evolving surface it is very simple to define the FLUX(1) and FLUX(2) respectively. More specific:

- if an element is active, the heat generation equation: 2.4 is applied combined with latent heat, in case it is a phase change.

- if it was found that boundary conditions must be applied to the element, then to this element the equation: 2.3 is applied, which is the equation of heat transfer with convection and radiation.

Regarding the elements that belong to the substrate, they are active from the beginning and we use the following ABAQUS keywords to handle the boundary conditions:

- FILM $\rightarrow$ Define film coefficients and associated sink temperatures.

- RADIATE $\rightarrow$ Specify radiation conditions in heat transfer analyses.

The material's thermal behavior is defined via the user subroutine UMATHT:

Listing (2.2) User subroutine interface (UMATHT)

```
1  SUBROUTINE UMATHT(U,DUDT,DUDG,FLUX,DFDT,DFDG,
2       1 STATEV,TEMP,DTEMP,DTEMDX,TIME,DTIME,PREDEF,DPRED,
3       2 CMNAME,NTGRD,NSTATV,PROPS,NPROPS,COORDS,PNEWDT,
4       3 NOEL,NPT,LAYER,KSPT,KSTEP,KINC)
5  C
6          INCLUDE 'ABA_PARAM.INC'
7  C
8          CHARACTER*80 CMNAME
```

```
 9            DIMENSION DUDG(NTGRD) ,FLUX(NTGRD) ,DFDT(NTGRD) ,
10          1 DFDG(NTGRD,NTGRD) ,STATEV(NSTATV) ,DTEMDX(NTGRD) ,
11          2 TIME(2) ,PREDEF(1) ,DPRED(1) ,PROPS(NPROPS) ,COORDS(3)
12
13
14           user coding to define U,DUDT,DUDG,FLUX,DFDT,DFDG,
15           and possibly update STATEV, PNEWDT
16
17
18           RETURN
19           END
```

where:

- U → Internal thermal energy per unit mass, U, at the end of increment.

- DUDT → Variation of internal thermal energy per unit mass with respect to temperature, evaluated at the end of the increment.

- FLUX(NTGRD) → Heat flux vector, at the end of the increment.

- DFDG(NTGRD,NTGRD) → Variation of the heat flux vector with respect to the spatial gradients of temperature, at the end of the increment.

These quantities are terms of the energy conservation equation: 2.2, which in combination with the boundary conditions in the UMATHT, define the thermal behavior of the material. It is also very important, in order to simulate the AM process, to set the specific heat and the thermal conductivity equal to zero for the inactive elements in the calculations above.

2.4 Mechanical analysis

2.4.1 UMAT

As it was mentioned earlier, the thermal analysis is executed first and after is completed, the mechanical analysis starts, using the temperature field that was computed in the thermal analysis.

In order, to define the mechanical behavior of the material, the UMAT user subroutine of ABAQUS is used. A quick overview of the UMAT:

Listing (2.3)   User subroutine interface (UMAT)

```
SUBROUTINE UMAT(STRESS,STATEV,DDSDDE,SSE,SPD,SCD,
     1 RPL,DDSDDT,DRPLDE,DRPLDT,
     2 STRAN,DSTRAN,TIME,DTIME,TEMP,DTEMP,PREDEF,DPRED,CMNAME,
     3 NDI,NSHR,NTENS,NSTATV,PROPS,NPROPS,COORDS,DROT,PNEWDT,
     4 CELENT,DFGRD0,DFGRD1,NOEL,NPT,LAYER,KSPT,JSTEP,KINC)
C
      INCLUDE 'ABA_PARAM.INC'
C
      CHARACTER*80 CMNAME
      DIMENSION STRESS(NTENS),STATEV(NSTATV),
     1 DDSDDE(NTENS,NTENS),DDSDDT(NTENS),DRPLDE(NTENS),
     2 STRAN(NTENS),DSTRAN(NTENS),TIME(2),PREDEF(1),DPRED(1),
     3 PROPS(NPROPS),COORDS(3),DROT(3,3),DFGRD0(3,3),DFGRD1(3,3),
     4 JSTEP(4)


      user coding to define DDSDDE, STRESS, STATEV, SSE, SPD, SCD
      and, if necessary, RPL, DDSDDT, DRPLDE, DRPLDT, PNEWDT


      RETURN
      END
```

where:

- DDSDDE(NTENS,NTENS)$\rightarrow$ Jacobian matrix of the constitutive model. DDSDDE(I,J) defines the change in the Ith stress component at the end of the time increment caused by an infinitesimal perturbation of the Jth component of the strain increment array.

- STRESS(NTENS)$\rightarrow$ This array is passed in as the stress tensor at the beginning of the increment and must be updated in this routine to be

the stress tensor at the end of the increment.

- STATEV(NSTATV)$\rightarrow$ An array containing the solution-dependent state variables.

2.4.2 UMAT flow and equations

The flow of UMAT is the following (with $\boldsymbol{\sigma}_n$:known):

$\rightarrow$ Form elastic stiffness: $\boldsymbol{\mathcal{L}}^e = 2G\boldsymbol{\mathcal{K}} + 3\kappa\boldsymbol{\mathcal{J}}$
$\rightarrow$ Check $\boldsymbol{F}_{n+1} - \boldsymbol{F}_n$, where $\boldsymbol{F}_n$: is the deformation gradient at the beginning of the increment and $\boldsymbol{F}_{n+1}$: is the deformation gradient at the end of the increment:

- if $\boldsymbol{F}_{n+1} - \boldsymbol{F}_n$=0:
  $\rightarrow$ Check YFLAG, where YFLAG is defined in the previous increment and defines if the material is in the elastic or plastic region:

  – if YFLAG=0 (elasticity):
    $\rightarrow$ $\boldsymbol{DDSDDE} = \boldsymbol{\mathcal{L}}^e = 2G\boldsymbol{\mathcal{K}} + 3\kappa\boldsymbol{\mathcal{J}}$ and $\boldsymbol{\sigma}_{n+1} = \boldsymbol{\sigma}_n$, where $\boldsymbol{DDSDDE}$ is the Jacobian Matrix.

  – if YFLAG=1 (plasticity):
    $\rightarrow$ $\boldsymbol{DDSDDE} = 2G\boldsymbol{\mathcal{K}} + 3\kappa\boldsymbol{\mathcal{J}} - \frac{4G^2}{3G+h}\boldsymbol{N} \otimes \boldsymbol{N}$ and $\boldsymbol{\sigma}_{n+1} = \boldsymbol{\sigma}_n$.

- if $\boldsymbol{F}_{n+1} - \boldsymbol{F}_n \neq 0$:
  $\rightarrow$ Compute: $\Delta\boldsymbol{\varepsilon}$, where: $\Delta\boldsymbol{\varepsilon} = \sum_{i=1}^{3} ln\lambda_i\boldsymbol{n_i} \otimes \boldsymbol{n_i}$, with λ_i: principal stretches and $\boldsymbol{n_i}$: principal stretch directions of $\Delta\boldsymbol{V}$,where: $\Delta\boldsymbol{V}^2 = \Delta\boldsymbol{F} \cdot \Delta\boldsymbol{F}^T$, $\Delta\boldsymbol{F} = \boldsymbol{F}_{n+1} \cdot \boldsymbol{F}_n^{-1}$
  $\rightarrow$ Compute: Φ, $\Phi = \sigma_e - \sigma_Y$, where σ_e is the equivalent von Mises stress and σ_Y is the yield strength.

  – if Φ>0 (plasticity):
    $\rightarrow$ $\boldsymbol{DDSDDE} = \boldsymbol{\mathcal{L}}^e - \frac{1}{L}(\boldsymbol{\mathcal{L}}^e : \boldsymbol{N})(\boldsymbol{\mathcal{L}}^e : \boldsymbol{N})$ and $\boldsymbol{\sigma}_{n+1} = \boldsymbol{\sigma}_n + \boldsymbol{\mathcal{L}}^e : \Delta\boldsymbol{\varepsilon} - 2G \, \Delta\bar{\varepsilon}^P \, \boldsymbol{N}$, where: $\boldsymbol{N} = \frac{3}{2\sigma_e}(\boldsymbol{\sigma}^e - \frac{\sigma_{kk}^e}{3}\boldsymbol{I})$, $\boldsymbol{\sigma}^e = \boldsymbol{\sigma}_n + \boldsymbol{\mathcal{L}}^e : \Delta\boldsymbol{\varepsilon}$ and $\sigma_e^e = \sqrt{\frac{3}{2}\boldsymbol{s}^e : \boldsymbol{s}^e}$.

  – if Φ<0 (elasticity):
    $\rightarrow$ $\boldsymbol{DDSDDE} = \boldsymbol{\mathcal{L}}^e$ and $\boldsymbol{\sigma}_{n+1} = \boldsymbol{\sigma}_n + \boldsymbol{\mathcal{L}}^e : \Delta\boldsymbol{\varepsilon}$.

It is important to highlight that the constitutive equations in the UMAT were build, using the backward Euler method.

2.4.3   UMAT extension for AM

The UMAT subroutine presented earlier is generally designed, to compute stresses and strains when mechanical loads applied to the body. So, it needs some extra features and changes, in order to simulate the AM process.
Some features are similar to those in the thermal analysis, as that for the inactive elements, the properties of the material are zero. More specific, for the Young's modulus (E) and the temperature difference (DTEMP1) between the time increment:

- check if the element is inactive.

- set E=0 and DTEMP1=0, if the element is inactive.

Of course this is combined with the MPC subroutine, that defines that all the inactive elements have not any displacement in all the directions.
The basic addition that UMAT needs is to consider the thermal loads, caused by the temperature differences. The resulting temperature field from the thermal analysis is used in the UMAT with the keyword: TEMPERATURE. So, the thermal deformations are calculated by the equation: 1.61 and then they are subtracted from the total deformations, in order to get the mechanical deformations, as it is shown in equations: 1.62-1.67. As a result, using the mechanical deformations in the UMAT, it will be calculated the mechanical stresses and strains, during the AM process.
Furthermore, it is known that the yield point of the material is a property that is affected by the temperature. So, it was added a subroutine to adjust the yield point along with the temperature. In this subroutine the following equation was used:

$$\sigma_y = \sigma_y - b(T - T_0) \tag{2.5}$$

where σ_y is the yield point, T is the temperature at that moment of time at the specific material point, T_0 is the temperature at the beginning of the analysis in that material point and b: is a coefficient, where for this specific mechanical analysis, was considered as b=0.28, as it works great with good results. There is not a specific value for this coefficient, this is an empirical

relationship.

So, with these changes in the UMAT, we were able to simulate the AM process and complete the model, that estimates the mechanical stresses and strains.

Chapter 3

Simulation of AM process, as applied to an AISI 316L austenitic stainless steel

3.1 Description of the application

Based on the formulation described in Chapter 2, a thermal analysis using diffusive heat transfer elements (DC2D4) was performed in order to evaluate the temperature evolution in the processed part, due to the successive material deposition. In the present work, a two-dimensional wall is built and a 15 mm x 14.5 mm substrate is used to start the metal deposition. The wall length is 10 mm and it is build by 10 layers of 0.5 mm height each. The substrate and wall model contains 1,070 DC2D4 elements and 1,162 nodes. For the mechanical analysis CPE4H elements was used.
The material of the application is an AISI 316L austenitic stainless steel and its properties are presented in table: 3.1.

Furthermore, we consider the following conditions for this application:

- Time of inactivity of the laser between successive layers: 10s.

- The speed of laser beam: 20 mm/s.

- Initial temperature: 27 ^oC.

- Laser power: 195 W.

density ($\frac{kg}{m^3}$) ρ	specific heat capacity ($\frac{kJ}{kg\ K}$) C_p (at T=300K)	thermal conductivity ($\frac{W}{m\ K}$) k (at T=300K)	film coefficient ($\frac{W}{m^2\ K}$) h
8,030	0.499	13.96	30

emissivity ε	latent heat of fusion ($\frac{kJ}{kg}$) Q_L	Young's Modulus (GPa) E	Yield point (MPa) σ_o
0.5	330	190	550

The solidus temperature (^oC) T_s	The liquidus temperature (^oC) T_l	Poisson's ratio v	thermal expansion coefficient ($^oC^{-1}$) a_{th}
1400	1459	0.3	1.6 x 10^{-5}

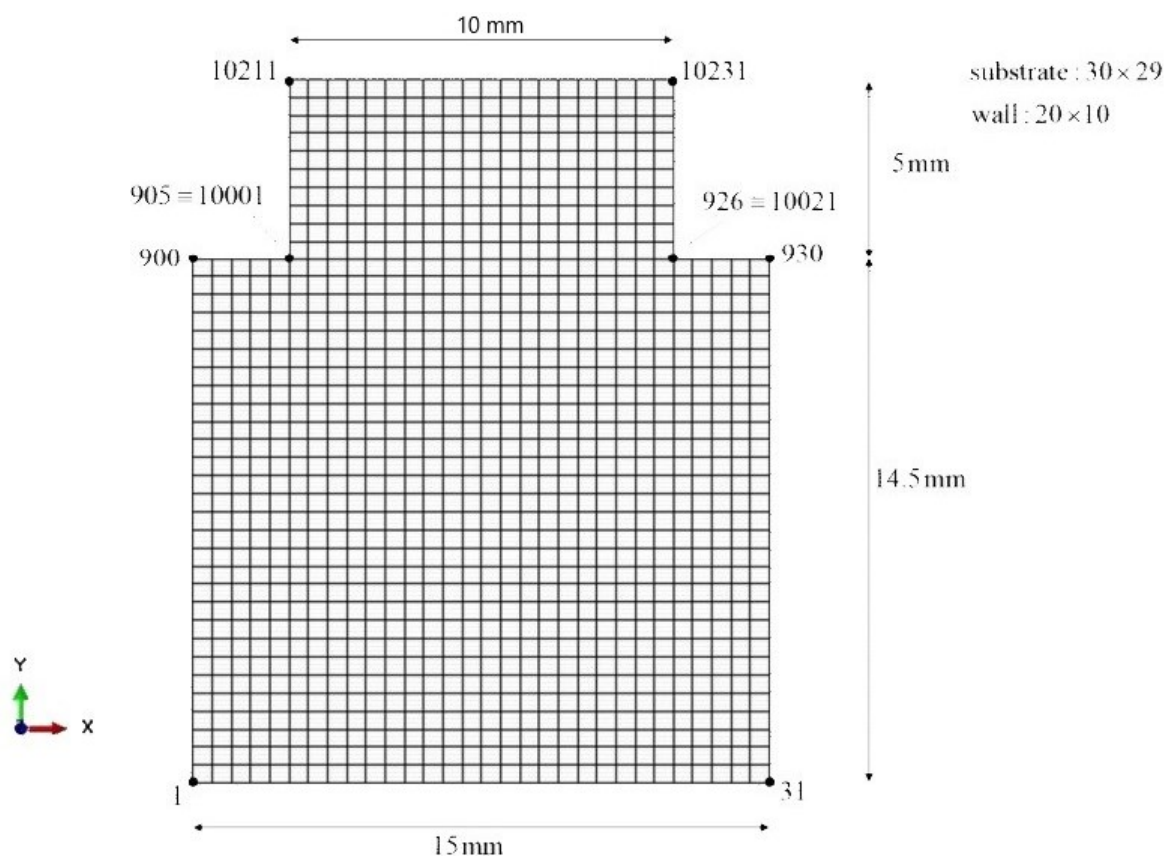| coefficient ($\frac{MPa}{^oC}$) b			
0.28			

Table (3.1)   Properties of the material

Figure (3.1)   Solid part and substrate geometry employed in the analysis.

- The laser starts from (x_0, y_0, z_0)=(2.5 mm, 14.5 mm, 0) and moves from left to right.

- The parameters of the volume of the ellipsoid of heat source: (a,b,c)=(1.5 mm, 0.9 mm, 1 mm).

Finally, the data of the figure: 3.2 was used, to change the values of specific heat capacity (C_p) and thermal conductivity (k), relatively with the change of the temperature, during the AM process.

So, in this simulation our goal is to create a wall using an additive manufacturing process, which consists of 10 layers, where the final shape of the body is presented in the figure: 3.1. First, the thermal analysis is completed and then the mechanical analysis is performed, using the temperature field extracted from the thermal analysis, in order to estimate the mechanical stresses and strains.

temperature (^oC) T	specific heat capacity ($\frac{kJ}{kg\ K}$) C_p	thermal conduc- tivity ($\frac{W}{m\ K}$) k	temperature (^oC) T	specific heat capacity ($\frac{kJ}{kg\ K}$) C_p	thermal conduc- tivity ($\frac{W}{m\ K}$) k
26.83	0.4987	13.96	1427.83	0.7699	17.98
126.83	0.5121	15.53	1526.83	0.7699	18.31
226.83	0.5255	17.1	1626.83	0.7699	18.64
326.83	0.5385	18.68	1726.83	0.7699	18.97
426.83	0.5519	20.25	1826.83	0.7699	19.3
526.83	0.5653	21.82	1926.83	0.7699	19.62
626.83	0.5786	23.39	2026.83	0.7699	19.95
726.83	0.5916	24.96	2126.83	0.7699	20.28
826.83	0.605	26.53	2226.83	0.7699	20.61
926.83	0.6184	28.1	2326.83	0.7699	20.94
1026.83	0.6318	29.67	2426.83	0.7699	21.26
1126.83	0.6448	31.25	2526.83	0.7699	21.59
1226.83	0.6849	32.82	2626.83	0.7699	21.92
1326.83	0.7699	34.39	2726.83	0.7699	22.25
1426.83	0.7699	35.96			

Table (3.2)   Changes of the C_p and k relatively with the change of the temperature.

3.2 Results

In this section the results of the application are presented. In figure: 3.2a, we can see the activation of the element 10110 (figure: 3.3). If the speed of the laser beam is 20 mm/s and between each layer is a 10 second break, as the element is the 10th element at the 6th layer, that means that it should be activated at: $5X(10 + 0.5) + (9X0.5 - 1.5)/20 = 52.65$ seconds. As we can see (figure: 3.2a) the element indeed is activated at 52.65 sec, after the starting of the process. Before that time the element is inactive. We can also see for the element 614 (figure: 3.3), which belongs to the substrate and it should be active from the beginning of the analysis. As we can observe in the figure: 3.2b, this is confirmed. So overall, the activation of the elements seems to function properly. In figure: 3.4, there are some frames of the activated elements during the AM process.

(a) element activation diagram for the element 10110

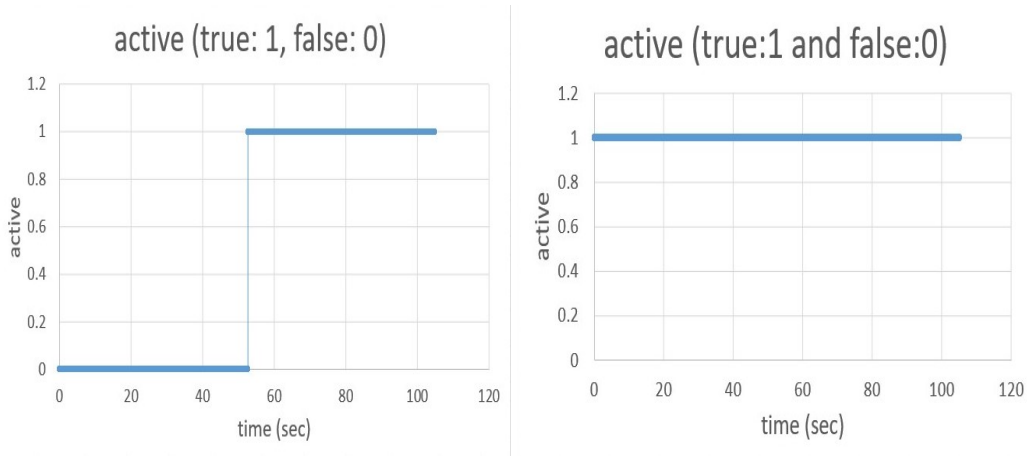(b) element activation diagram for the element 614

Figure (3.2)   Activation diagrams

Subsequently, we examine the temperature variation for different nodes of the structure. The temperature field in AM is highly transient as well as spatially non-uniform. Figure: 3.5 represents the variation of the temperature along with time for different nodes of the structure. First of all, we can very easily observe the thermal cycles, when the laser beam is active
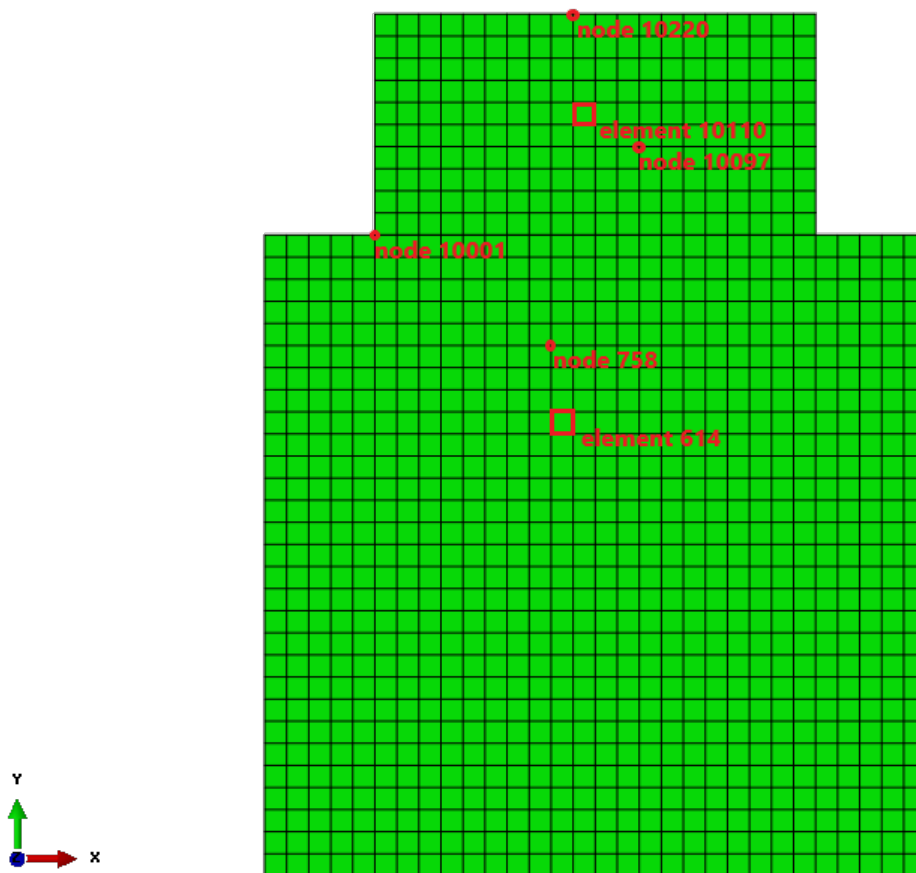
Figure (3.3)   Solid part and substrate geometry where the selected nodes and elements are highlighted in red

(a) t=0 sec

(b) t=0.45 sec

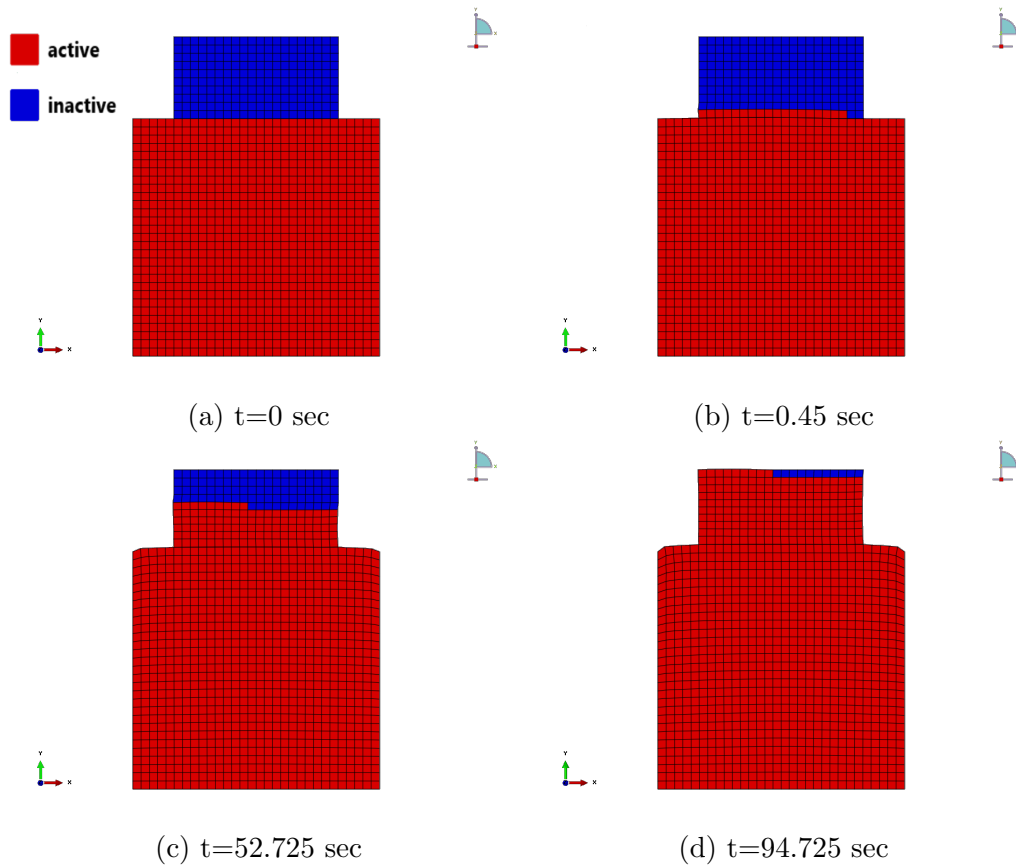(c) t=52.725 sec

(d) t=94.725 sec

Figure (3.4)   Different timestamps in a row of the activated elements

the temperature increases and when it pauses to cool off, the temperature drops to a new higher low. It is clear that as we move in a higher layer node, the higher the peak temperature gets. Furthermore, for the node: 758 (see Fig: 3.3), as it belongs to the substrate and it does not come in contact with the laser beam, the temperature increases gradually to its peak, as more heat is transferred in the body during the AM process. In contrast, the other nodes (see Fig: 3.3) of the wall reach their peak temperature at the beginning of their activation, as the laser beam transfers them a lot of heat, when it passes over them. Figure: 3.6 shows the temperature distribution for different timestamps, where the peak temperature is the highest at the pool center and decreases gradually with distance away from the center. In AM the substrate acts as a heat sink. Therefore, for the upper layers, heat transfer through the substrate decreases, which in turn, effectively increases

the peak temperature for the upper layers. Because of the rapid scanning of laser beam the temperature contours are elongated behind the heat source and compressed in front of the beam. The highly transient and spatially non-uniform temperature distribution, that shown in Figure: 3.6, is responsible for the generation of the stress and strain fields.
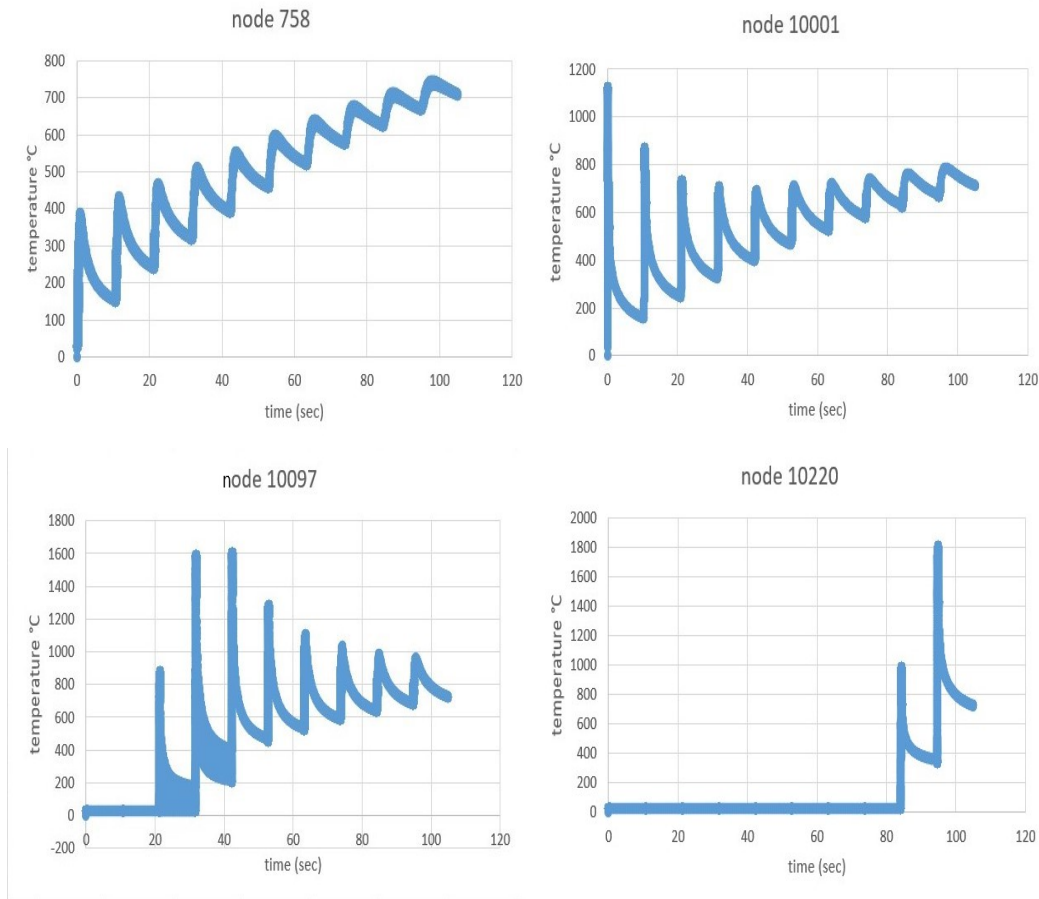

Figure (3.5)   Temperature variation (^{o}C) for multiple nodes

Finally, we present the results of the mechanical analysis. Figure: 3.8 represents the stresses distribution across the structure at different timestamps. Evolution of stresses depends on the transient temperature distribution especially during cooling of the body. Although, the peak temperature is the
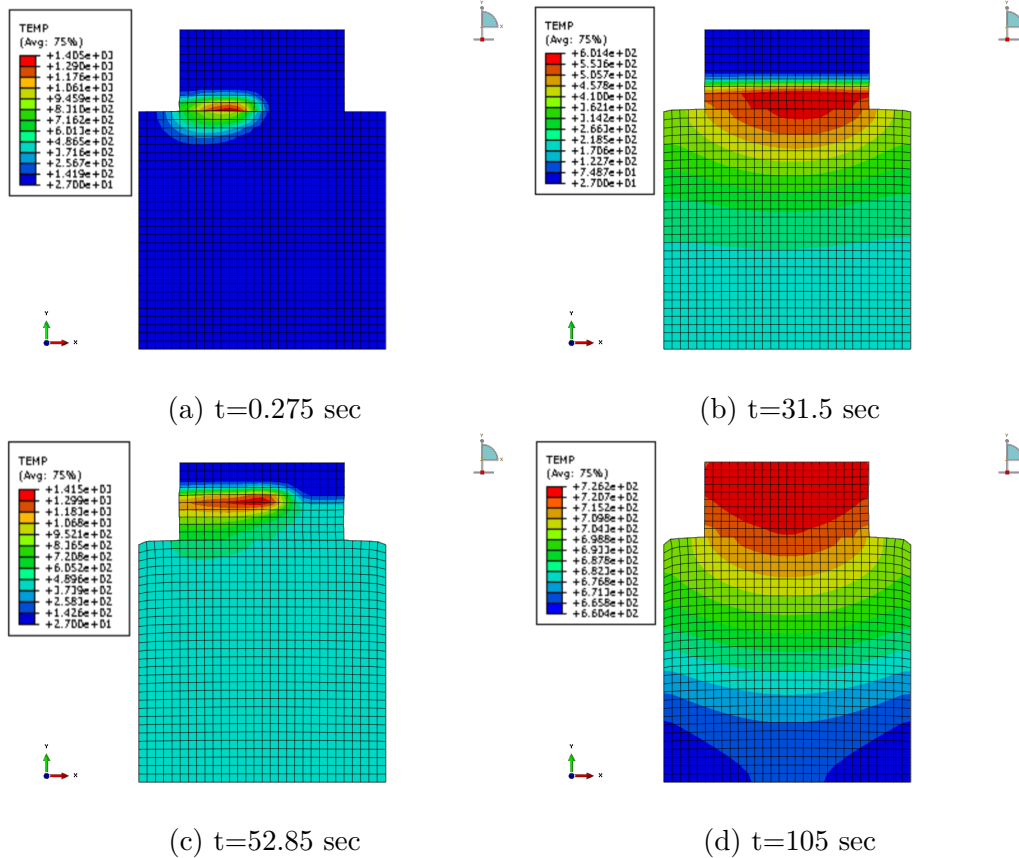
(a) t=0.275 sec   (b) t=31.5 sec

(c) t=52.85 sec   (d) t=105 sec

Figure (3.6)   Temperature variation (^{o}C) for different timestamps in a row

highest at the pool center, we observe that does not result to the highest stresses. This seems reasonable, as the high temperature softens the material locally and lowers the yield strength, so the magnitude of stress is relatively low as it is limited by the the yield strength at the high temperature. Furthermore, the location of the maximum stresses, after the cool off period, are near the top of the wall (figure: 3.9). As the temperature, decreases gradually from top to bottom of the structure, when it cools off, it would be normal for the stresses to follow a similar pattern. However, we can observe a small region underneath the top layers, with lower stresses than the rest of the body, as it is shown in figure: 3.9. This happens because there, the temperature is high enough to soften the material, but not so high to develop high stresses, as a result we see lower stresses in that region. In figure: 3.8, we can observe the deformation at the sides of the wall, as more

and more layers are added and the obvious plastic deformation of the upper edges of the substrate, that is totally explained by the high stresses that are developed in these regions. In figure: 3.7, we have a clear view of the deformation of the body, as it is compared the designed and the actual shape of the body. So, clearly the substrate is elongated in the y-axis, due to tensile loads and the wall is compressed in the y-axis, due to compressive loads.
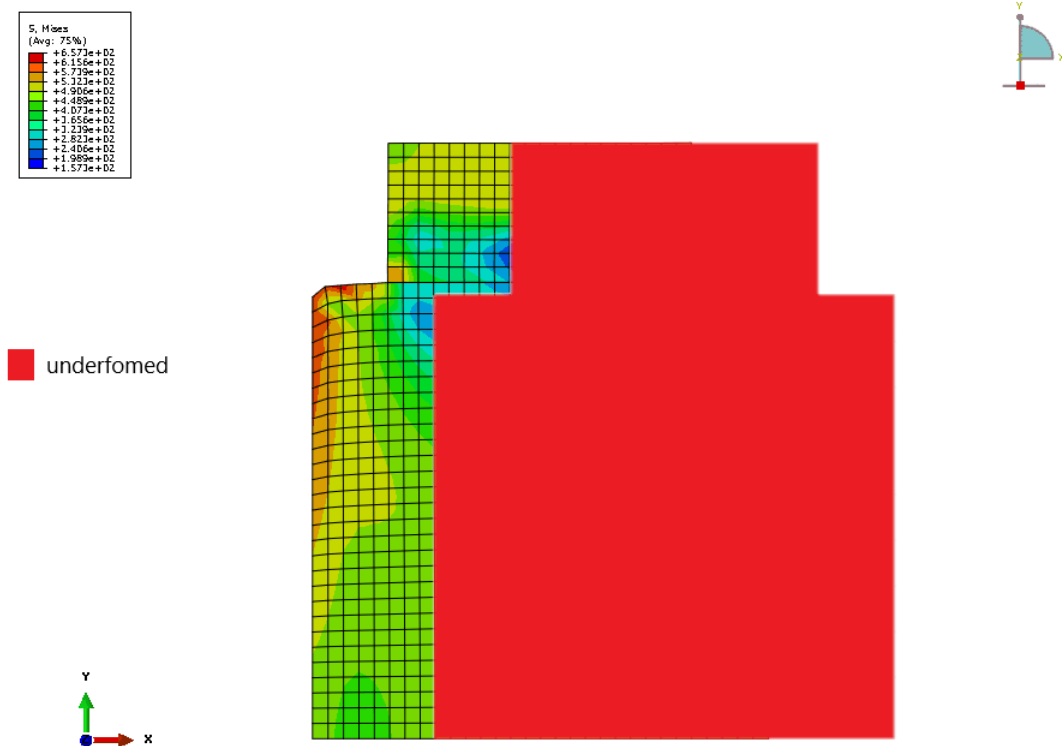

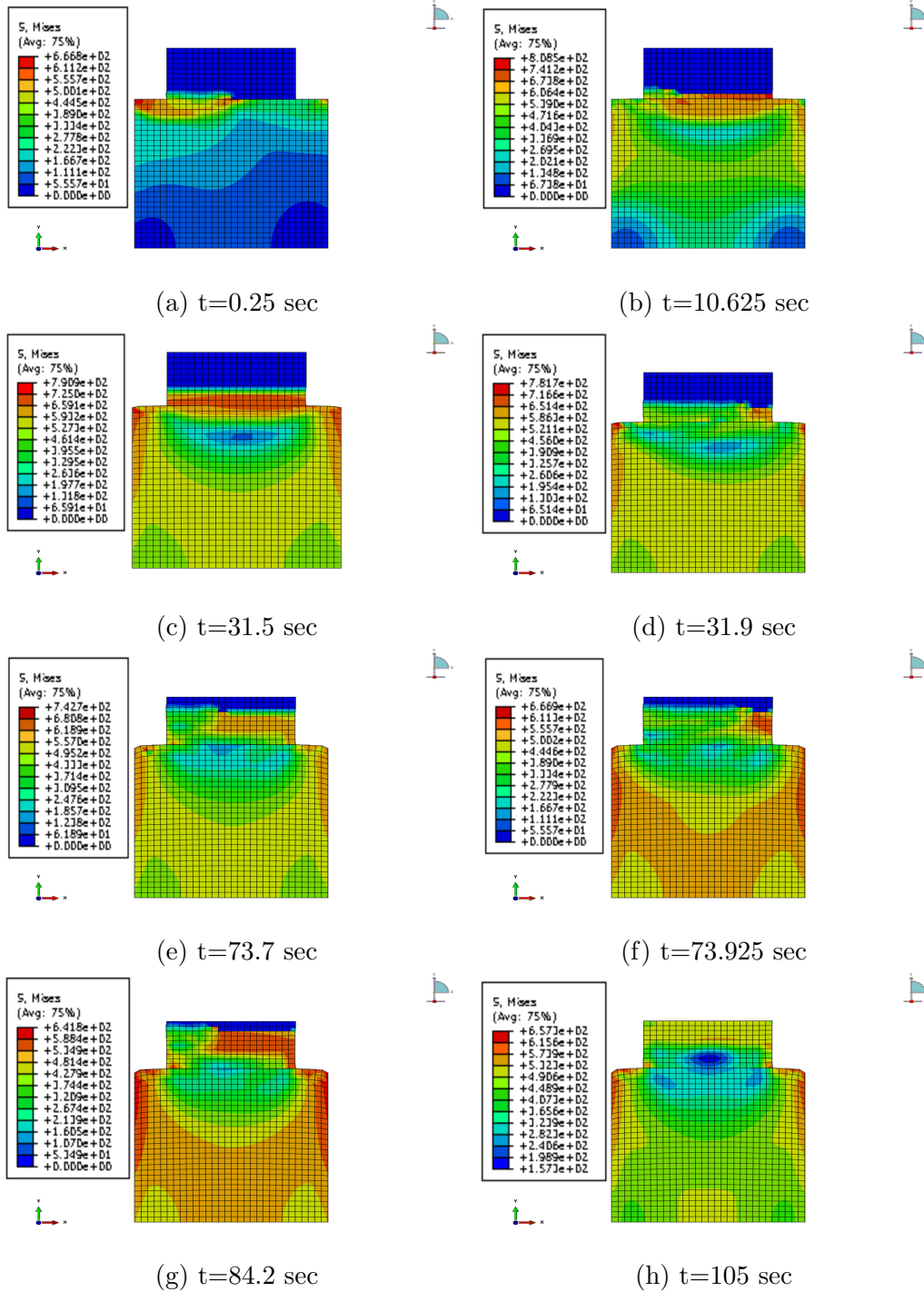Figure (3.7)   Comparison between the designed and the actual shape of the body

(a) t=0.25 sec

(b) t=10.625 sec

(c) t=31.5 sec

(d) t=31.9 sec

(e) t=73.7 sec

(f) t=73.925 sec

(g) t=84.2 sec

(h) t=105 sec

Figure (3.8)   Distribution of the stresses (MPa) during the AM process

(a) Stress field (t=21.425 sec)

(b) Strength yield distribution (t=21.425 sec)

(c) Stress field (t=21.5 sec)

(d) Strength yield distribution (t=21.5 sec)

(e) Stress field (t=26.5 sec)

(f) Strength yield distribution (t=26.5 sec)

(g) Stress field (t=31.5 sec)

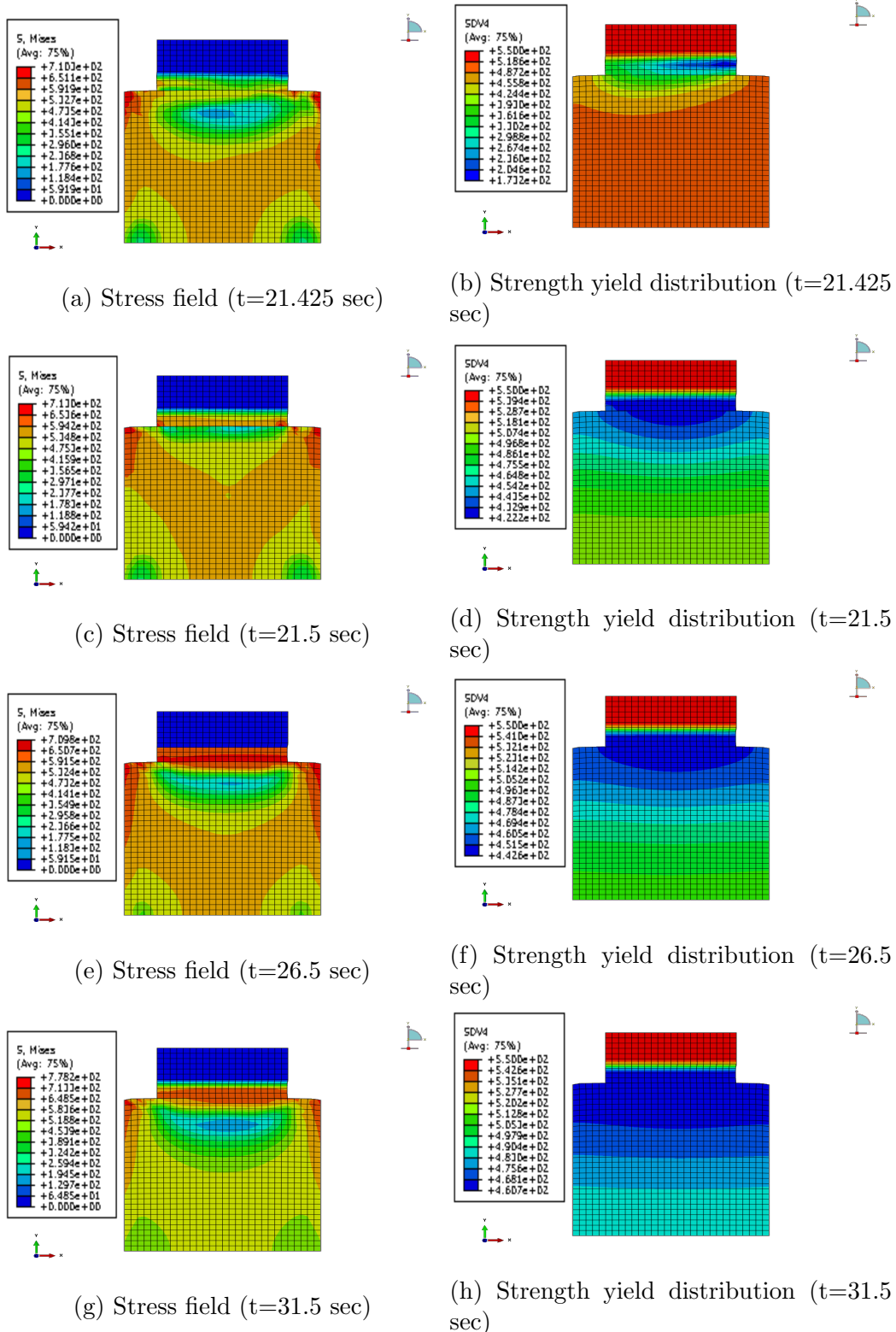(h) Strength yield distribution (t=31.5 sec)

Figure (3.9)   Distribution of the stresses and yield strength (MPa) during cool of period of the third layer

Closure

In this thesis additive manufacturing of an AISI 316L austenitic stainless steel was studied via an integrated thermomechanical modeling approach. A finite element technique was employed to evaluate the temperature evolution due to successive material deposition. The ensuing temperature field was provided as an input for a mechanical finite element analysis to calculate, based on local mechanical properties, the residual stresses and distortions. The primary purpose was to develop a methodology which simulates accurately the AM process.

We can summarize the results we saw in the previous section as follows:

- The activation of the elements simulates perfectly the movement of the laser beam.

- The combination of the correct element activation and the MPC user subroutine work, so the inactive elements indeed do not affect the analysis, which is also completed in reasonable computation time. As we can observe that for the inactive elements the temperature remains at: 27^oC and the stresses are equal to zero.

- The temperature distribution of the material seems to be accurate, as the elements of the wall reach the peak temperature at the beginning of their activation where the heat source hits them, while the elements of the substrate reach their peak temperature gradually as the heat flows from the wall to the substrate. We can also clearly note the fluctuation of the temperature for each element in response to the thermal cycles of the laser beam.

- Finally, we can observe the successful coupling of the thermal and mechanical behavior of the material, as the stresses respond according to

the temperature field. The stresses are increased gradually for the elements at the substrate along with the temperature and the stresses around the molten pool get very high, as we have the highest temperatures, but not in the molten pool, as the yield strength gets to low and the material becomes too soft and limits the stresses.

We can also conclude from the results that during the AM process, residual stresses are developed and because of the stresses the body is deformed significantly.
Finally, we close with some recommendations for future work, which could improve this work:

- Switch from a 2-d model to a 3-d model.

- Evaluate the results of the mechanical stresses and strains estimation with results from an actual experiment.

- Tune the parameters of the model to eliminate the residual stresses arising from the AM process.

Bibliography

[1] ABAQUS, Analysis User's Manual, Version 6.14, ©Dassault Syst´emes, 2014.

[2] Aravas N., 'Cartesian Tensors', University of Thessaly Publications (2005).

[3] A. Vasinonta, J.L. Beuth, M. Griffith, Process maps for predicting residual stress and melt pool size in the laser-based fabrication of thin-walled structures, J. Manuf. Sci. Eng. 129 (2007) 101–109.

[4] M.P. Mughal, H. Fawad, R.A. Mufti, M. Siddique, Deformation modelling in layered manufacturing of metallic parts using gas metal arc welding: effect of process parameters, Model. Simul. Mater. Sci. Eng. 13 (2005) 1187.

[5] A.H. Nickel, D.M. Barnett, F.B. Prinz, Thermal stresses and deposition patterns in layered manufacturing, Mater. Sci. Eng. A 317 (2001) 59–64.

[6] S. Ghosh, J. Choi, Three-dimensional transient finite element analysis for residual stresses in the laser aided direct metal/material deposition process, J. Laser Appl. 17 (2005) 144–158.

[7] G. Vastola, G. Zhang, Q.X. Pei, Y-W. Zhang, Controlling of residual stress in additive manufacturing of Ti6Al4V by finite element modeling, Addit. Manuf. (2016) 231-239.

[8] Z. Nie, G. Wang, J.D. McGuffin-Cawley, B. Narayanan, S. Zhang, D. Schwam, M. Kottman, Y.K. Rong, Experimental study and modeling of H13 steel deposition using laser hot-wire additive manufacturing, J. Mater. Process. Technol. 235 (2016) 171–186.

[9] Panagiotis Michaleris, Modeling metal deposition in heat transfer analyses of additive manufacturing processes, Finite Elements in Analysis and Design Volume 86 (2014) 51-60.

[10] John H. Lienhard IV and V, A Heat transfer textbook (2019).

[11] Yunus A. Cengel, Heat transfer, McGraw-Hill (2nd edition) (2002).

[12] Rohan Abeyaratne, Continuum Mechanics, MIT publications (1988).

[13] D. S. Chandrasekharaiah and Lokenath Debnath, Continuum Mechanics, Academic Press (1994).

[14] W Michael Lai, Erhard Krempl, David Rubin, Introduction to continuum mechanics, Butterworth-Heinemann (1996).

[15] J. Chakrabarty, Theory of Plasticity, Butterworth-Heinemann (third edition) (2012).

[16] C. Li1, C.H. Fu1, Y.B. Guo1, F.Z. Fang2, Fast Prediction and Validation of Part Distortion in Selective Laser Melting, Procedia Manufacturing (2015) 355-365.

[17] T. Mukherjee a, W. Zhang b, T. DebRoy, An improved prediction of residual stresses and distortion in additive manufacturing, Computational Materials Science (2017) 360-372.

[18] J.C. Heigel a, P. Michaleris a, E.W. Reutzel b, Thermo-mechanical model development and validation of directed energy deposition additive manufacturing of Ti–6Al–4V, Additive Manufacturing (2015) 9-19.

[19] J. Ding, P. Colegrove, J. Mehnen, S. Ganguly, P.M. Sequeira Almeida, F. Wang, S. Williams, Thermo-mechanical analysis of Wire and Arc Additive Layer Manufacturing process on large multi-layer parts, Computational Materials Science (2011) 3315-3322.

[20] X. Shan, C.M. Davies, T. Wangsdan, N.P. O'Dowd, K.M. Nikbin, Thermo-mechanical modelling of a single-bead-on-plate weld using the finite element method, International Journal of Pressure Vessels and Piping (2008) 110-121.

[21] Riqing Ye, John E. Smugeresky, Baolong Zheng, Yizhang Zhou, Enrique J. Lavernia, Numerical modeling of the thermal behavior during the LENS® process, Materials Science and Engineering: A (2006) 47-53.

[22] L. Costa, R. Vilar, T. Reti, A.M. Deus, Rapid tooling by laser powder deposition: Process simulation using finite element analysis, Acta Materialia (2005) 3987-3999.

[23] https://gctbooks.files.wordpress.com/2016/02/heat-transfer-a-practical-approach-by-y-a-cengel.pdf, page 68, Figure 2-13.

[24] https://www.researchgate.net/profile/Sasa-Mitrovic/publication/292527228/figure/fig7/AS:640239253069824@1529656341035/Motion-of-a-continuum-body.png.